



# Gene co-expression network analysis of the heat-responsive core transcriptome identifies hub genes in *Brassica rapa*

Lixin Yue<sup>1</sup> · Guoliang Li<sup>1</sup> · Yun Dai<sup>1</sup> · Xiao Sun<sup>1</sup> · Fei Li<sup>1</sup> · Shifan Zhang<sup>1</sup> · Hui Zhang<sup>1</sup> · Rifei Sun<sup>1</sup> · Shujiang Zhang<sup>1</sup>

Received: 18 November 2020 / Accepted: 16 April 2021 / Published online: 27 April 2021  
© The Author(s), under exclusive licence to Springer-Verlag GmbH Germany, part of Springer Nature 2021

## Abstract

**Main conclusion** Gene co-expression network analysis of the heat-responsive core transcriptome in two contrasting *Brassica rapa* accessions reveals the main metabolic pathways, key modules and hub genes, are involved in long-term heat stress.

**Abstract** *Brassica rapa* is a widely cultivated and economically important vegetable in Asia. High temperature is a common stress that severely impacts leaf head formation in *B. rapa*, resulting in reduced quality and production. The purpose of this study was thus to identify candidate heat tolerance genes by comparative transcriptome analysis of two contrasting *B. rapa* accessions in response to long-term heat stress. Two *B. rapa* accessions, ‘268’ and ‘334’, which showed significant differences in heat tolerance, were used for RNA sequencing analysis. We identified a total of 11,055 and 8921 differentially expressed genes (DEGs) in ‘268’ and ‘334’, respectively. Functional enrichment analyses of all of the identified DEGs, together with the genes identified from weighted gene co-expression network analyses (WGCNA), revealed that the autophagy pathway, glutathione metabolism, and ribosome biogenesis in eukaryotes were significantly up-regulated, whereas photosynthesis was down-regulated, in the heat resistance of *B. rapa* ‘268’. Furthermore, when *B. rapa* ‘334’ was subjected to long-term high-temperature stress, heat stress caused significant changes in the expression of certain functional genes linked to protein processing in the endoplasmic reticulum and plant hormone signal transduction pathways. Autophagy-related genes might have been induced by persistent heat stress and remained high during recovery. Several hub genes like *HSP17.6*, *HSP17.6B*, *HSP70-8*, *CLPB1*, *PAP1*, *PYR1*, *ADC2*, and *GSTF11* were discussed in this study, which may be potential candidates for further analyses of the response to long-term heat stress. These results should help elucidate the molecular mechanisms of heat stress adaptation in *B. rapa*.

**Keywords** *Brassica rapa* · DEGs · Key modules · Long-term heat stress · Metabolic pathways · RNA-seq

## Abbreviations

CK	Control treatment
DEGs	Differentially expressed genes
FPKM	Fragments per kilo-base per million reads
GO	Gene ontology enrichment
HSF	Heat shock transcription factor
HSP	Heat shock protein

HT	Heat stress treatment
KEGG	Kyoto encyclopedia of genes and genomes
RC	Recovery treatment
WGCNA	Weighted gene co-expression network analysis

## Introduction

*Brassica rapa* L. (Brassicaceae) originated in China and is a widely cultivated and economically important vegetable in Asia (Dai et al. 2020). It is adapted to cooler temperatures, with an optimum growth temperature of 12–25 °C. In recent years, the frequent occurrence of extremely high temperatures caused by global warming has become one of the most significant abiotic stresses limiting global crop yields (Challinor et al. 2014; Awasthi et al. 2015; Ray et al. 2015).

Communicated by Dorothea Bartels.

Lixin Yue, Guoliang Li have contributed equally to this work.

✉ Shujiang Zhang  
Zhangshujiang@caas.cn

<sup>1</sup> Institute of Vegetables and Flowers, Chinese Academy of Agricultural Sciences, Zhongguancun, Nandajie No. 12, Haidian District, Beijing 100081, People’s Republic of China

When suffering from heat stress, the early-maturing *B. rapa* cultivar cannot form or lose the leafy head, which then leads to degradation of the products, thus affecting output (Sato et al. 2002). Therefore, investigating the molecular mechanisms of heat stress should benefit growth, development, and breeding in *B. rapa*.

In order to survive under, and adapt to, heat stress conditions, plants have evolved numerous inherent tolerance mechanisms, including several putative heat sensors, heat shock transcription factors (HSFs), and heat shock factors and proteins (HSPs) response pathways, as well as a network of phytohormones and secondary metabolites (Bokszczanin et al. 2013; Qu et al. 2013). Upon exposure to heat, plants first sense and transduce heat stress signals. Several putative heat sensors have been proposed, including a plasma membrane cyclic nucleotide gated calcium channel and two unfolded protein sensors in the endoplasmic reticulum and the cytosol (Liu et al. 2015). In addition, many HSFs and HSPs play crucial parts in heat tolerance. The HSFs belong to a family of transcription factors conserved throughout eukaryotes that bind to downstream genes encoding transcription factors, enzymes, and chaperone proteins (Ohama et al. 2017). HSFs, as the central regulators, also regulate the expression of HSP genes (Liu et al. 2015; Guo et al. 2016). It was reported that HSPs function in various cellular processes, including protein folding, assembly, translocation, and degradation (DeRocher et al. 1991). A variety of phytohormones, such as auxin, abscisic acid (ABA), ethylene (ET), and salicylic acid (SA), are also involved in thermotolerance. They function in plant growth and development and act as the watchdogs of the stress response (Verma et al. 2016). Moreover, plants can adapt to stressful conditions by producing metabolites. Changes in temperature alter the expression of metabolites by influencing the physiology and metabolism of plants (Isah 2019). For example, it is reported that diverse primary and secondary metabolic pathways, including glycolysis, pentose phosphate pathway, isoprenoid biosynthesis, and the metabolisms of amino acid, fatty acid, nucleotide, and vitamins, are involved in heat tolerance in spinach (Li et al. 2019).

Additionally, reactive oxygen species (ROS) and autophagy have a great impact on the heat response. ROS play a dual role in plant biology, acting on the one hand as important signal transduction molecules and on the other as toxic byproducts of aerobic metabolism that accumulate in cells during different stress conditions. Several HSFs have been reported to participate in ROS gene network regulation during abiotic stress (Miller et al. 2008). Autophagy can help alleviate heat stress, and autophagosomes were found to accumulate in *Arabidopsis* and tomato plants exposed to heat stress (Zhou et al. 2013, 2014; Avin-Wittenberg 2019).

Many studies have investigated heat stress in *B. rapa*. In *B. rapa*, heat-responsive miRNA and nat-siRNAs have been

identified, and some of these small RNAs are upregulated under heat stress (Yu et al. 2012). At least 30 *BrHsf* genes have been identified and are classified into three groups (A, B, C) (Song et al. 2014; Huang et al. 2015). Quantitative real-time-PCR (qRT-PCR) analysis of the heat-sensitive material ‘Chiifu-401-42’ showed that 23 *BrHsf* genes were obviously upregulated under 38 °C heat treatment at 1 h (Song et al. 2014). In another study, an orthologous gene interaction network was constructed and included five genes (*MBF1C*, *ROF1*, *TBP2*, *CDC2*, and *HSP70*) that are closely related to heat stress in *B. rapa* (Huang et al. 2015). The exogenous *Arabidopsis* *HTT2* gene was overexpressed in *B. rapa*, resulting in an increase in the thermotolerance of transgenic lines (Dong et al. 2015). Eleven genes involved in normal growth and chloroplast development were differentially expressed between the two accessions ‘Chiifu’ and ‘Kenshin’ and conferred differing heat resistance to these *B. rapa* accessions (Lee et al. 2018). Other studies have evaluated exposure to heat stress in other vegetables, such as pepper (*Piper nigrum* L.) (Li et al. 2014), eggplant (*Solanum melongena* L.) (Zhang et al. 2018a), and spinach (*Spinacia oleracea* L.) (Qi et al. 2019).

With the recent development of high-throughput sequencing technology, RNA sequencing (RNA-Seq) has become a powerful tool for exploring the genes involved in abiotic stress and has been widely applied in numerous horticultural crops. WGCNA can be used to identify modules, which are composed of genes with consistent expression patterns and that are highly correlated with some external sample traits (Langfelder and Horvath 2008). Using RNA-Seq and WGCNA analyses, the molecular mechanisms of abiotic stress have been increasingly elucidated in *Arabidopsis* (*Arabidopsis thaliana* (L.) Heynh.), grapevine (*Vitis vinifera* L.), maize (*Zea mays* L.), rice (*Oryza sativa* L.), broccoli (*Brassica oleracea* L. var. *italica* Plenck), and others (Amrine et al. 2015; Hopper et al. 2016; Kost et al. 2017; Tan et al. 2017; Lin et al. 2019). However, to date, no studies have evaluated heat stress in *B. rapa* using RNA-Seq and WGCNA analyses in order to elucidate the molecular mechanism of the long-term heat stress response.

In this study, we aimed to systematically determine the response mechanism of two *B. rapa* accessions differing in their heat tolerance to heat stress and recovery, as well as identify key genes involved in this response. To this end, we utilized RNA-Seq and WGCNA analysis to construct a gene interaction network of *B. rapa* and identify the biological and metabolic pathways, core heat-stress responsive modules, and core genes under heat stress treatments of different durations. Here, we generated a comprehensive and integrated dataset that provides guidance for the breeding of new accessions with elevated heat tolerance and offers a theoretical basis for future studies on the regulatory mechanisms of heat tolerance in *B. rapa*.

## Materials and methods

### Plant materials and heat treatment

The two *B. rapa* (*Brassica rapa* L. ssp. *pekinensis*) materials used in the experiments were ‘B18♂’ (268), a heat-resistant highly inbred line, and ‘A04’ (334), a heat-sensitive highly inbred line. These two accessions were collected and bred by the Institute of Vegetables and Flowers, Chinese Academy of Agricultural Sciences, Beijing. Seeds of each line were grown in a nursery greenhouse. Plants were initially grown at  $25 \pm 2$  °C with a photoperiod of 16/8 h light/dark,  $150 \text{ mol/m}^2/\text{s}^1$  light intensity, and a relative humidity of 60%. For treatment, 30-day-old plants were exposed to heat stress conditions at 40 °C/30 °C (light/dark) for 10 days, following which they were subjected to recovery at 25 °C for 4 days. During the period of heat treatment, the seedlings were watered daily. For the control, the plants were maintained under non-stress conditions at 25 °C/18 °C (light/dark) for 14 days.

### Sample collection and RNA sequencing

In the 40 °C heat stress treatment, leaf samples were sampled at 0, 2, 4, 6, 8, and 10 days after treatment. In the recovery treatment at 25 °C, leaf samples were then sampled at 2 and 4 days. The control plants, which were sampled daily for 14 days, were sampled at the same time as the treatment plants. The functional leaves (the third fully-expanded leaves from the center of each seedling) were collected in a single biological replicate. The three biological replicates included three separate sets of heat stress and non-stress treatment experiments. Samples were frozen in liquid nitrogen and stored at  $-80$  °C until RNA extraction. A defined code was used to standardize the sample names: starting with the initial letter ‘S’, the first three numbers of each sample indicate the different breeding line (268 = ‘B18♂’; 334 = ‘A04’), the following two letters indicate the type of treatment (CA = control; HT = heat stress treated; RC = recovery), the seventh digit represents the days of different treatments (0 = 0 days; 2 = 4 days; 4 = 8 days; 5 = 10 days; 7 = 14 days), and the last two numbers represent the biological replicate (01, 02, or 03).

Total RNA was extracted from the leaf samples using TRIzol reagent (Invitrogen, Carlsbad, CA, USA) following the manufacturer’s protocol. The purity, concentration, and integrity of the RNA samples were tested using advanced molecular biology equipment to ensure the use of qualified samples for transcriptome sequencing. According to the manufacturer’s instructions, the mRNA-Seq libraries were

constructed using the Illumina TruSeq RNA Sample Preparation Kit (Illumina, New England Biolabs, Ipswich, MA, USA) with insert sizes of  $200 \pm 25$  bp for each sample. The libraries were then sequenced to generate paired-end transcriptome reads on the Illumina HiSeq 2000 platform provided by Biomarker Technologies Corporation, Beijing.

### Transcriptome analysis

The *B. rapa* reference genome sequence (v3.0) and annotation files were downloaded from the Brassica Database (<http://brassicadb.cn/#/Download/>) (Cheng et al. 2011; Zhang et al. 2018a). Clean data were obtained by removing reads containing adapters, reads containing poly-N, and low-quality reads from the raw data using in-house Perl scripts. At the same time, the Q20, Q30, GC-content, and sequence duplication level of the clean data were calculated. All of the downstream analyses were based on high-quality clean data. The clean reads were then aligned to the *B. rapa* reference genome sequence using Tophat v2.0.9 (Trapnell et al. 2009). The values of fragments per kilo-base per million reads (FPKM) in each sample were estimated and normalized by Cufflinks v2.2.1 (Trapnell et al. 2012).

### Differential gene expression analysis

The DESeq R package (<http://www.bioconductor.org/packages/release/bioc/html/DESeq.html>) was used to conduct differential expression analysis of three groups (three biological replicates per group) (Love et al. 2014). The false discovery rate (FDR) was controlled using the Benjamini and Hochberg (1995) approach to adjust the *P*-values. Genes with an adjusted *P*-value  $< 0.01$  identified by DESeq2 were assigned as differentially expressed (Anders and Huber 2010).

### Gene annotations and enrichment analysis

The Gene Ontology (GO) annotation was performed in GOseq R (Young et al. 2010). The GO enrichment analysis of DEGs was performed in R Studio (R version 3.6.2). The genome ID of *B. rapa* was used as a query in the GO annotation using GOseq R. Gene functions were annotated based on the Swiss-Prot, EuKaryotic Orthologous Groups (KOG)/Clusters of Orthologous Groups (COG), KEGG Orthology (KO), Pfam, and Non-redundant (Nr) NCBI databases.

### Gene co-expression network analysis and visualization

The DEGs were used as an input in the R package WGCNA to construct gene co-expression networks (Langfelder and Horvath 2008). Those genes, obtained by setting the FPKM ( $\text{FPKM} \geq 1$ ; variation of  $\text{FPKM} \geq 0.5$ ),

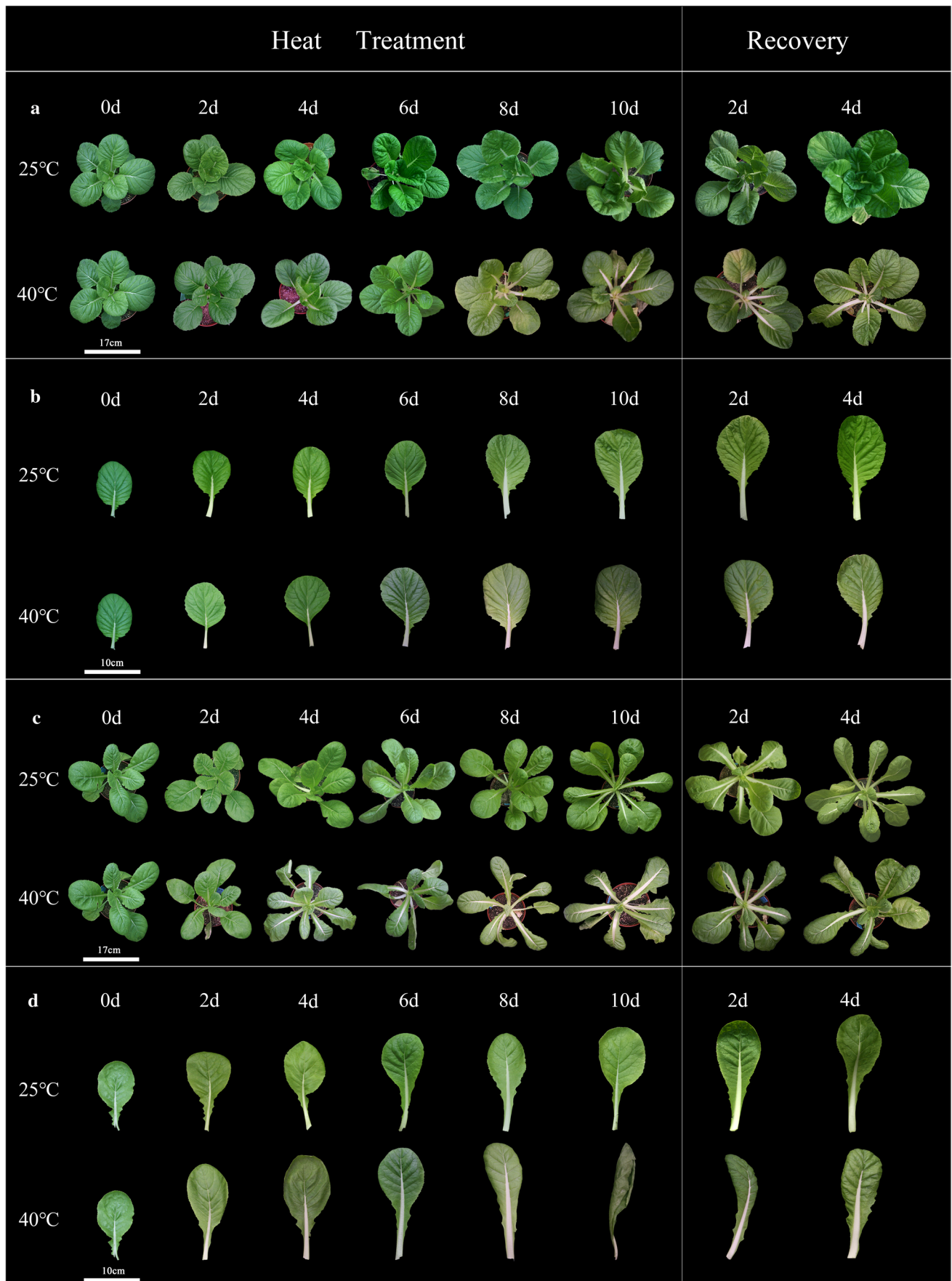


**Fig. 1** Typical phenotypes of a heat-resistant plant ‘268’ (a, b) and heat-sensitive plant ‘334’ (c, d) under 25 °C and 40 °C for 10 days, followed by recovery at 25 °C for 4 days

were screened for co-expression network construction. A total of 7422 DEGs were selected in ‘268’ for co-expression network construction, whereas 5684 DEGs were selected in ‘334’. The following parameters were used to obtain weighted co-expression clusters, which were regarded as ‘modules’: weighted network = unsigned, hierarchical clustering tree = dynamic hybrid tree cut algorithm, power = 10, minimum module size = 30, minimum height for merging modules = 0.25.

Module eigengenes were used to summarize the module profiles and were combined with the trait data, which were the first principal component in the expression matrix. Pearson’s correlation coefficient was used to calculate the correlation between the module eigengene and two *B. rapa* samples from different treatments. The correlation is reflected by the depth of the color in the heatmap.

Hub genes were regarded as the characteristic representation of each module and showed the most connections in the co-expression network. The numbers of edges were also used for measuring hubness: the more edges in a node, the higher the hubness of the gene. The edge numbers were positively related to the absolute  $k_{ME}$  values.  $k_{ME}$ , defined as the eigengene-based connectivity for each gene, was calculated based on the Pearson’s correlation coefficients between the expression level and the module eigengenes. Hub genes were assigned according to both the  $k_{ME}$  value and edge numbers (Xie et al. 2019). The top 20 hub genes were calculated and ranked based on the MCC method using the novel Cytoscape plugin *cytoHubba* (Chin et al. 2014).

### Validation of candidate hub genes by qRT-PCR

The expression analysis for validation of candidate hub genes was validated by qRT-PCR. The Bio-Rad CFX96 RT-PCR Detection system (Bio-Rad, Hercules, CA, USA) and SYBR Green II PCR Master mix (Takara, Nojihigashi, Kusatsu, Japan) were used for the qRT-PCR reactions. The qRT-PCR was performed with three technical replicates as described previously (Han et al. 2019). The housekeeping gene, *ACTIN*, was considered as the internal control and gene expression data were analyzed using the  $2^{-\Delta\Delta C_t}$  method (Livak and Schmittgen 2001). SPSS v22.0 (SPSS, Chicago, IL, USA) was used to perform the analysis of variance (ANOVA), and the significance threshold was  $P < 0.05$ . Excel 2016 (Microsoft, Redmond, WA, USA) was used to visualize and plot the results.

### Data availability

The raw RNA-Seq data are available from the NCBI SRA database under the accession number PRJNA663233.

## Results

### Typical heat-responsive plants and heat-sensitive plant accessions

In order to assess the morphological effect of high temperature on heat-resistant and heat-sensitive *B. rapa* accessions, we performed 15 different treatments, namely CK 0 days, CK 2 days, CK 4 days, CK 6 days, CK 8 days, CK 10 days, CK 12 days, CK 14 days, HT 2 days, HT 4 days, HT 6 days, HT 8 days, HT 10 days, RC 2 days, and RC 4 days. Compared with the control of the same period, the treatment plants showed different degrees of heat damage symptoms, such as leaf shrinkage and curling, leaf chlorosis, plant growth stagnation, and plant wilt and death (Fig. 1a–d). During the period of exposure to high temperature, ‘268’ showed no significant heat damage symptoms compared with ‘334’ plants. The only symptoms included leaf greening and yellowing, elongation of the petioles, and an open rosette structure (Fig. 1a, b). From Fig. 1c, it is evident that the entire plant of 334 exhibited obvious heat damage symptoms from the fourth day of the high-temperature treatment. The leaves began to shrink and warp, the petioles became elongated, the leaves outgrew their pots, and the plant displayed an open rosette structure (Fig. 1d). With the extension of the heat treatment, plant growth became slowly restricted, with fewer leaf numbers recorded. The degree of shrinkage and curling of the leaves increased, and the green leaves faded and became increasingly yellow (Fig. 1d). On the 10th day of heat stress at 40 °C, the leaves were dehydrated and had shrunk and wilted (Fig. 1d). When recovered at 25 °C for 2 days, the damage caused by heat stress was clearly alleviated. When recovered at 25 °C for 4 days, the drooping plants had revived and had recovered to close to that of the control plants. The results indicated that ‘334’ was more sensitive to heat stress than ‘268’, and high temperature would have a greater effect on these heat stress-susceptible accessions.

### RNA sequencing analysis

To investigate the transcriptome dynamics between the heat-tolerant and heat-sensitive *B. rapa*, we performed RNA-Seq experiments using total RNA isolated from the nine treatments from the ‘268’ and ‘334’ accessions. All of the treatments were analyzed in three independent biological replicates (54 samples in total). A total of

2,989,714,630 raw reads and 446.28 Gb clean data were generated from ‘268’ and ‘334’, respectively (Table S1). The Q30 was  $\geq 93.85\%$ , the average GC content was 47.98%, and the read alignment rate ranged from 86.85% to 92.66% (Table S1). The clean reads were mapped to the *B. rapa* reference genome (v3.0). Then the mapped files were processed via HISAT2 and String Tie software, which generated a consensus transcriptome assembly with a total of 47,690 genes, including 44,161 known genes and 3529 new genes.

The uniquely mapped reads for each sample (Table S2) were processed using String Tie to identify the numbers of transcripts as the FPKM value. Genes with normalized reads above 1.0 FPKM were used for the analysis (Table S3; Table S4). Approximately 31% of expressed genes were in the 0.5–5 FPKM range, and 63% of the expressed genes were in the 5–100 FPKM range (Fig. 2a). The principal component analysis (PCA) and Pearson’s correlation analysis suggested that there was a good correlation between the biological replicates of each treatment of the two *B. rapa* accessions (Fig. 2b, c). Overall, we concluded that the quality of our RNA-Seq data was high and the sequencing depth was sufficient for further analysis, and there was sufficient

variation between the samples and different treatment conditions to identify DEGs.

### Comparisons of DEGs under different heat stress treatments

The DEGs for the different heat stress and subsequent recovery conditions were identified according to an expression level  $\log_2(\text{fold-change}) > 1$  and  $\text{FDR} < 0.01$  in each pairwise comparison. We detected a total of 19,976 DEGs in both the genotypes, of which 11,055 and 8921 DEGs were observed in ‘268’ and ‘334’, respectively (Fig. 3). After analyzing the gene expression of the five treatment groups, we compared the groups with the same treatment durations and different treatment temperatures. In *B. rapa* ‘268’, a total of three (one up-regulated genes and two down-regulated genes), 5559 (2782 up-regulated genes and 2777 down-regulated genes), 7222 (3808 up-regulated genes and 3414 down-regulated genes), and 591 (253 up-regulated genes and 338 down-regulated genes) DEGs were detected in ‘CK-4 vs. HT-4’, ‘CK-8 vs. HT-8’, ‘CK-10 vs. HT-10’, and ‘CK-14 vs. RC-4’, respectively (Fig. 3a). These results showed that the number of DEGs continued to increase at 4, 8, and 10 days of exposure to heat stress, while that of the DEGs decreased

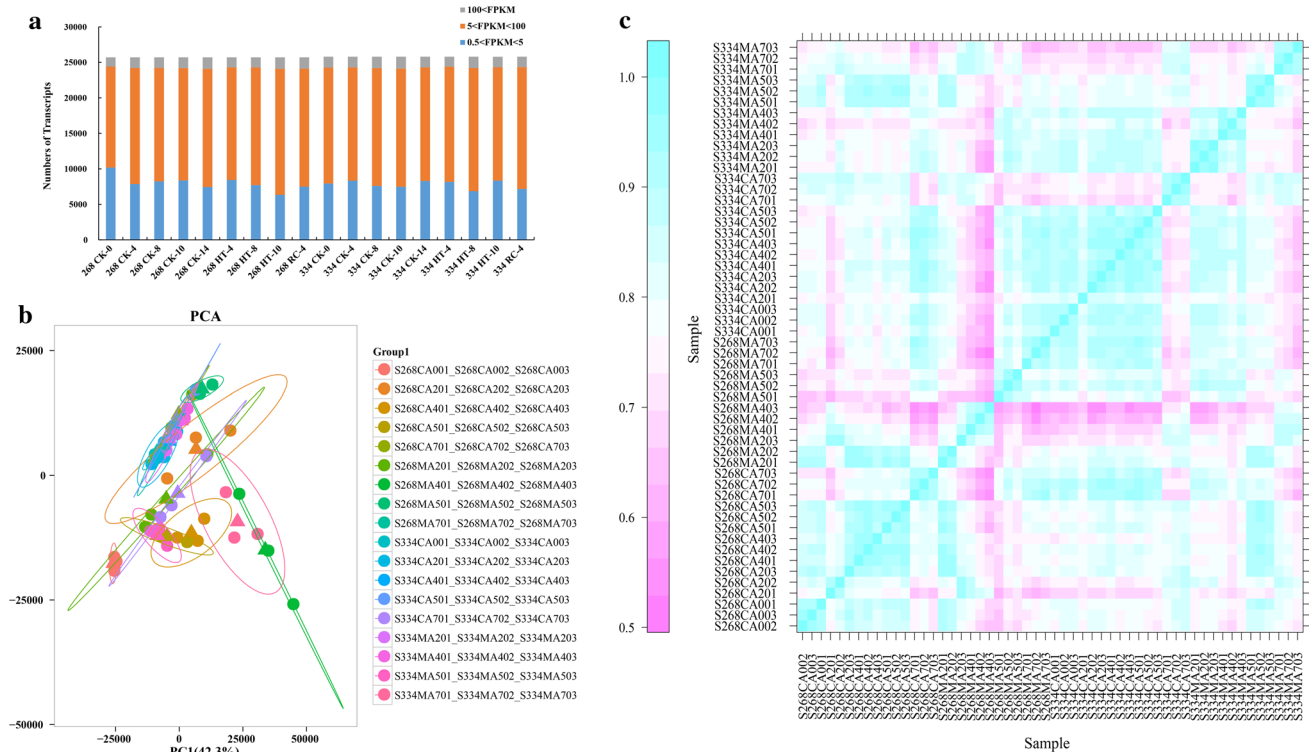


**Fig. 2** Good correlation between the biological replicates of each treatment of the two *B. rapa* accessions. **a** Bar graph showing the numbers of detected transcripts in each sample. Different colors represent different ranges of FPKM-values. **b** Principal component anal-

ysis (PCA) of the RNA-Seq data. Each color represents a group of treatments that belong to the same cluster. **c** Cluster dendrogram of different samples. The color scale (blue to purple) indicates correlation between samples

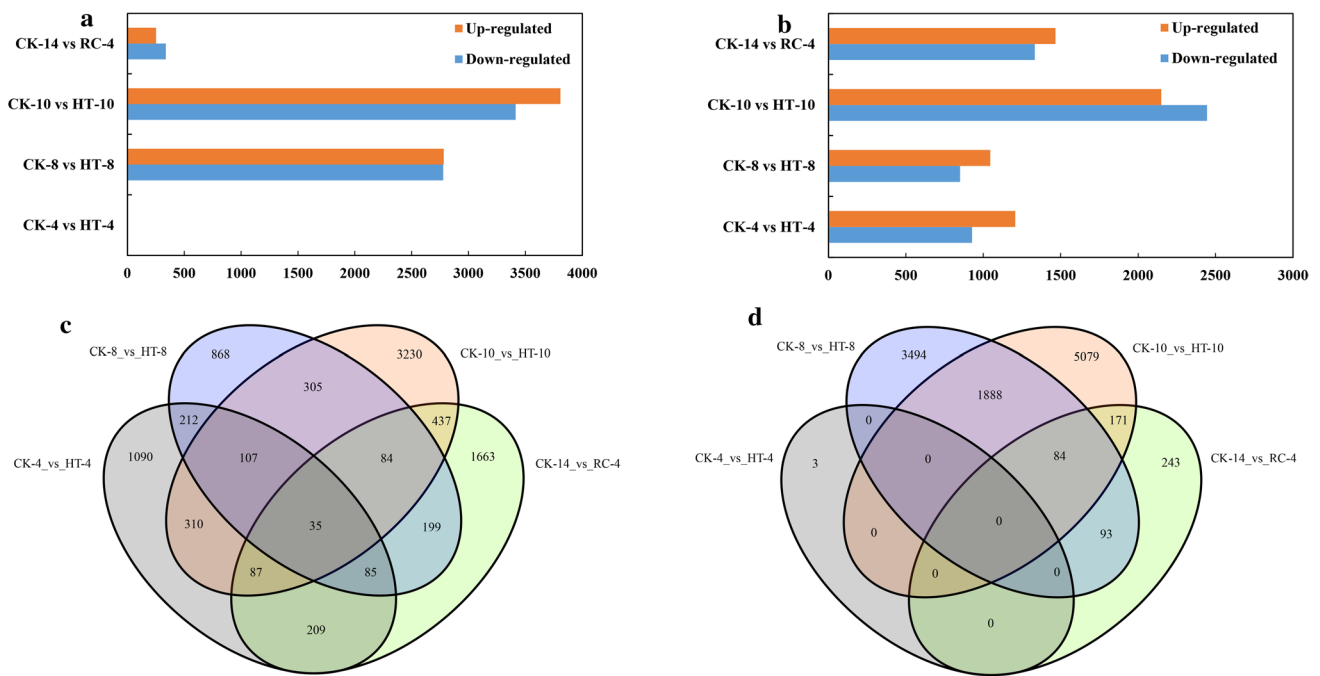


**Fig. 3** Gene expression profile of different *B. rapa* genotypes under heat stress. **a, b** Numbers of DEGs in each comparison between the heat response treatment (c) and its simultaneous control treatment between heat-resistant *B. rapa* ‘268’ (a) and heat-sensitive *B. rapa* ‘334’ (b), respectively. **c, d** Venn diagrams of differentially expressed genes (DEGs) between heat-resistant *B. rapa* ‘268’ (c) and heat-sensitive *B. rapa* ‘334’ (d). Orange represents the up-regulated genes, and blue represents the down-regulated genes. Notes: First, CK-0,

CK-4, CK-8, CK-10, and CK-14 represent *B. rapa* seedlings treated at 25 °C for 0, 4, 8, 10, and 14 days, respectively. Second, HT-4, H-8, and HT-10 represent *B. rapa* seedlings treated at 40 °C for 4, 8 and 10 days, respectively. Third, RC-4 represent *B. rapa* seedlings treated at 40 °C for 10 days and then recovered at 40 °C for 4 days. FDR < 0.01 and  $\log_2$  FCI > 1 were used as cut-off criteria for significance

during the recovery process. In *B. rapa* ‘334’, a total of 2135 (1207 up-regulated genes and 928 down-regulated genes), 1895 (1045 up-regulated genes and 850 down-regulated genes), 4595 (2150 up-regulated genes and 2445 down-regulated genes), and 2799 (1466 up-regulated genes and 1333 down-regulated genes) DEGs were detected in ‘CK-4 vs. HT-4’, ‘CK-8 vs. HT-8’, ‘CK-10 vs. HT-10’, and ‘CK-14 vs. RC-4’, respectively (Fig. 3b). Compared with the ‘CK-8 vs. HT-8’ treatment stage, the number of DEGs was greater than in the ‘CK-4 vs. HT-4’ treatment stage (Fig. 3b). The ‘CK-10 vs. HT-10’ treatment stage had the greatest number of DEGs (Fig. 3b). Our results also indicated that a greater number of genes participated in the heat stress recovery of ‘334’ (Fig. 3a, b). Furthermore, from the Venn diagram, we also detected DEGs at each comparison belonging to either unique or overlapping sets (Fig. 3c, d). Most DEGs (5079; 70.33%) in the comparison of ‘CK-10 vs. HT-10’ were unique to HT-10. Additionally, 3494 DEGs (41.12%) in the comparison of ‘CK-4 vs. HT-4’ were unique to HT-4, and 243 DEGs (62.85%) in the comparison of ‘CK-10 vs. HT-10’ were unique to RC-4. However, no significant DEGs were found for the intersection of ‘CK-4 vs. HT-4’, ‘CK-8 vs. HT-8’, and ‘CK-10 vs. HT-10’. Similarly, 1869, 1459, 3911,

and 2459 DEGs were also unique to HT-4, HT-8, HT-10, and RC-4 in *B. rapa* ‘334’.

### Functional enrichment analysis of identified DEGs unique to each pairwise treatment

GO enrichment and Kyoto Encyclopedia of Genes and Genomes (KEGG) analyses were performed to identify heat stress-related genes involved in the key biological processes and metabolic pathways associated with the heat response. In *B. rapa* ‘268’, three DEGs (*BraA03g005630.3C*, *BraA05g026340.3C*, and *BraAnng003260.3C*) were found at the ‘CK-4 vs. HT-4’ treatment stage. *BraA03g005630.3C*, which was significantly down-regulated, was annotated as NAC domain-containing protein 83 and responded to ABA and leaf senescence during the heat stress period (Table S3). At the ‘CK-8 vs. HT-8’ treatment stage, KEGG pathway analysis (Fig. S1a) showed that 2782 up-regulated genes were mainly enriched in valine, leucine, and isoleucine degradation, glutathione metabolism, limonene and pinene degradation, and regulation of autophagy. Most of the 2777 down-regulated genes were significantly enriched

in ribosome, biosynthesis of amino acids, glucosinolate biosynthesis, and photosynthesis (Fig. S1b). At the ‘CK-10 vs. HT-10’ treatment stage, most of 3808 up-regulated genes were significantly involved in ribosome biogenesis in eukaryotes, and most of the 3414 down-regulated genes were significantly enriched in photosynthesis, photosynthesis-antenna proteins, carbon metabolism, and protein processing in the endoplasmic reticulum (Fig. S1c, d). During recovery, pathways including glyoxylate and dicarboxylate metabolism, iron fixation in photosynthetic organisms, and plant hormone signal transduction were up-regulated in the 253 DEGs (Fig. S1e). Secondary metabolite biosynthesis processes, such as cutin, suberine, and wax biosynthesis and linoleic acid metabolism, were significantly down-regulated in the 338 DEGs (Fig. S1f). In addition, GO analysis identified that the significantly enriched biological processes contributed by these DEGs were relatively consistent with the metabolic pathways (Fig. S2).

In *B. rapa* ‘334’, during the ‘CK-4 vs. HT-4’ stage, our detailed metabolic pathway analysis suggested that the 1207 up-regulated DEGs were mainly enriched in the following pathways: circadian rhythm-plant, sulfur metabolism, and carotenoid biosynthesis (Fig. S3a). Additionally, 928 down-regulated DEGs were enriched in plant–pathogen interaction, ether lipid metabolism, and starch and sucrose metabolism (Fig. S3b). Furthermore, none of the 1045 up-related DEGs were significantly enriched in any biological metabolic pathway during the ‘CK-8 vs. HT-8’ stage, while 850 down-regulated DEGs were mainly enriched in phenylpropanoid biosynthesis, phenylalanine metabolism, flavonoid biosynthesis, fatty acid elongation, and plant hormone signal transduction (Fig. S3c, d). At the ‘CK-10 vs. HT-10’ stage, photosynthesis, photosynthesis-antenna proteins, and sulfur metabolism were up-regulated in 2150 up-related DEGs, and cutin, suberine, and wax biosynthesis were down-regulated in 2445 DEGs (Fig. S3e, f). After a long period of high-temperature stress, biological processes such as glutathione metabolism and ribosome biogenesis eukaryotes during the recovery period were significantly up-regulated, and plant hormone signal transduction, photosynthesis-antenna proteins, and protein processing in the endoplasmic reticulum were down-regulated (Fig. S3g, h). Therefore, the heat response was characterized by decreased lipid metabolism, plant hormone signal transduction, carbohydrate metabolism, secondary metabolism, and photosynthetic processes. We further identified that the most abundant term in the biological process category of up-regulated DEGs was ‘response to heat’ when *B. rapa* ‘334’ subjected to 4-day heat stress (Fig. S4). However, the biological process ‘response to heat’ was suppressed upon exposure to 10 days of heat stress and 4 days of recovery under normal conditions (Fig. S5).

## Construction of gene co-expression networks

To investigate the gene expression response to heat-stress and obtain a comprehensive understanding of the molecular mechanism of thermotolerance in the two *B. rapa* accessions, we performed a co-expression network analysis for the DEGs using the WGCNA software package. After filtering out the genes with low abundance and low variability (FPKM < 1), 7422 DEGs in ‘268’ and 5684 DEGs in ‘334’ remained and were used in the WGCNA. The co-expression network was constructed based on the pairwise correlation of gene expression in 27 samples of each of ‘268’ and ‘334’. Modules were defined as clusters of highly interconnected genes with high correlation coefficients between genes in the same cluster. If the number of genes in the module was less than 30, the module was not considered. The analysis of ‘268’ identified 13 different modules, as shown in the dendrogram of Fig. 4a. The target gene number of each module ranged from 41 to 3007 (Fig. 4b). Each module is marked with a different color, and the main branches define these modules. As shown in the dendrogram, the 13 modules produced by the WGCNA of ‘334’ could distinguished by different colors (Fig. 4c), and the number of target genes in each module ranged from 49 to 2210 (Fig. 4d).

WGCNA was used to comprehensively display gene expression levels on a network scale. We also focused on the expression profiles of individual DEGs. We performed an expression gene display for each processing stage of the two *B. rapa* lines, corresponding to each module (Fig. S6). The enrichment and differential expression analysis from the co-expression network module showed very similar characteristics.

To further assess the relationships between different modules, the eigengenes of the modules were calculated in each sample set (Fig. S7). The eigengenes showed a significantly positive correlation in some module pairs. For example, MEdarkturquoise was positively correlated with MEivory, MEpaleturquoise, MEsalmon, and MEwhite in ‘268’. Moreover, MEMagenta also showed a significantly positive correlation with the other colored modules such as MEwhite, MEfloralwhite, and MEtan. Similarly, MELightcyan was also closely related with MEdarkturquoise and MEblue in *B. rapa* ‘334’. MERoyalblue was also positively correlated with MEpurple, MEcyan, and MEgrey 60.

## Certain co-expression networks identified seven key modules obviously correlated with heat stress and recovery in the two genotypes of *B. rapa*

The different heat stress durations resulted in obviously different module–trait relationships (MTRs). Each module formed by WGCNA contained positively and negatively correlated genes, and the expression level changed between the



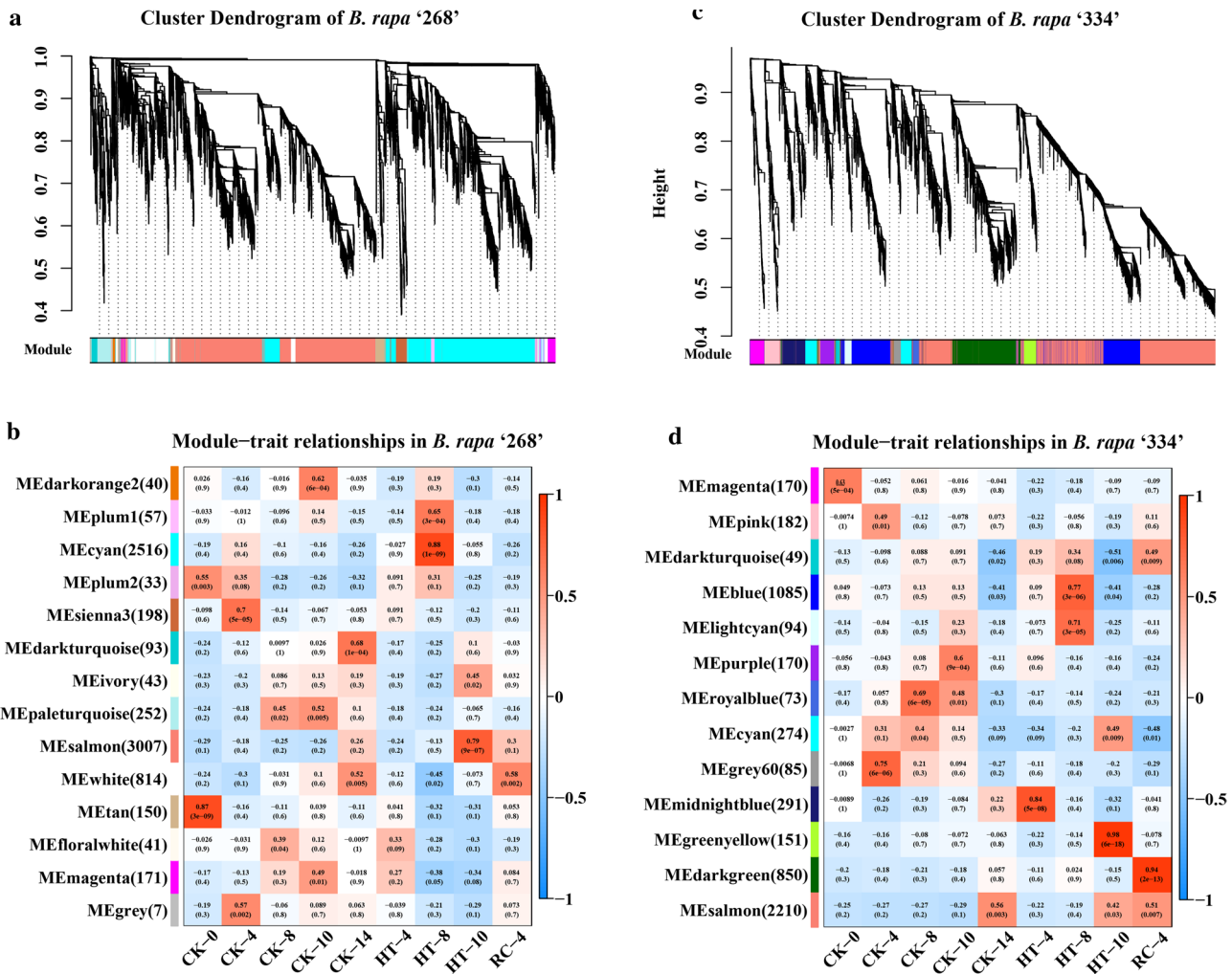


**Fig. 4** Co-expression network analysis of the DEGs and module-trait relationships (MTRs) in the two *B. rapa* accessions in response to heat-stress. **a** Hierarchical clustering tree of 27 samples in *B. rapa* '268' showing the gene co-expression modules identified by WGCNA. The branches constitute 13 modules labeled in different colors. **b** Relationships between modules (left) and traits (bottom) in *B. rapa* '268'. The numbers in brackets on the left show the number

of genes in a module. Red and blue represent positive and negative correlations, respectively. The darker colors indicate higher correlation coefficients. Numbers represent Pearson's correlation coefficient  $r^2$  values and the  $P$ -value for the correlation (in brackets). **c** Hierarchical clustering tree of 27 samples identified 13 gene co-expression modules in *B. rapa* '334'. **d** Relationships between modules (left) and traits (bottom) in *B. rapa* '334'

different treatments. Modules with MTR > 0.7 were selected as representatives of the two *B. rapa* accessions for further analysis. Figure 4b shows the correlations from -1 (blue) to 1 (red). MEtan ( $r^2 = 0.87$ ,  $P = 3e-09$ ) was positively correlated with 'CK-0' (25 °C, 0 days) in '268'. There were no significant correlations in 'HT-4' (40 °C, 4 days), suggesting that the gene expression profiles at 4 days after heat stress treatment did not vary widely. Additionally, MEcyan ( $r^2 = 0.88$ ,  $P = 1e-9$ ) showed a remarkable correlation with 'HT-8' (40 °C, 8 days), while MESalmon ( $r^2 = 0.79$ ,  $P = 9e-07$ ) was positively correlated with 'HT-10' (40 °C, 10 days). These results suggested that the gene expression levels in each group may increase under long-term heat stress treatment. In addition, some modules also showed a

high correlation with the control treatment. For example, MEsienna3 ( $r^2 = 0.7$ ,  $P = 5e-05$ ) was positively correlated with 'CK-10' (25 °C, 10 days).

Similarly, we explored the MTRs in '334'. As shown in Fig. 4d, there were significant correlations between MEGrey60 ( $r^2 = 0.75$ ,  $P = 6e-06$ ) and 'CK-0' (25 °C, 0 days). MEMidnightblue ( $r^2 = 0.84$ ,  $P = 5e-08$ ) was highly related to 'HT-4' (40 °C, 4 days). MEblue ( $r^2 = 0.77$ ,  $P = 3e-06$ ) and MElightcyan ( $r^2 = 0.71$ ,  $P = 3e-05$ ) displayed a significant correlation with 'HT-8' (40 °C, 8 days). MEgreenyellow ( $r^2 = 0.98$ ,  $P = 6e-18$ ) showed an extremely strong correlation with 'HT-10' (40 °C, 10 days). Additionally, MEdarkgreen ( $r^2 = 0.94$ ,  $P = 2e-13$ ) was highly correlated with 'RC-4' (25 °C, 4 days recovery). Notably, there were no

modules highly correlated with ‘RC-4’ in ‘268’. Compared with ‘268’, more modules were positively correlated with different treatments, especially the heat stress treatment. By constructing co-expression networks and exploring the module–trait relationships, seven key modules were obviously correlated with heat stress and recovery in the two genotypes of *B. rapa*. Two key modules (MEcyan and MEsalmon) were detected in *B. rapa* ‘268’ and five modules (MEMidnightblue, MEblue, MELightcyan, MEGreenyellow and MEDarkgreen) were obtained in *B. rapa* ‘334’, of which four of them were highly related to different heat stress durations and one responded to recovery.

### GO and KEGG enrichment analysis of the detected co-expressed modules

Eigen modules are genes that are representative of gene groups with highly correlated expression levels. We identified two eigen modules in *B. rapa* ‘268’, including MEcyan (HT-8) and MEsalmon (RC-4), and five eigen modules in *B. rapa* ‘334’, including MEMidnightblue (HT-4), MELightcyan and MEblue (HT-8), MEGreenyellow (HT-10), and MEDarkgreen (RC-4), by calculating the correlations between modules and traits (Fig. 4).

To reveal the specific functions of each co-expressed module, we performed GO and KEGG analysis of DEGs from each module separately. GO analysis indicated that ‘flavonoid biosynthetic process’ and ‘response to chitin’ were the most significantly enriched biological processes in ‘268’MEcyan (Fig. S8a). KEGG analysis indicated ‘glutathione, amino acid metabolism and degradation’ and ‘regulation of autophagy’ as the most significantly enriched metabolic pathways, suggesting that genes in the blue module contribute to heat tolerance by regulating glutathione, amino acid metabolism, and degradation and autophagy (Fig. S8b). Regarding ‘268’MEsalmon, GO analysis identified ‘RNA modification’ as the most significantly enriched biological process, which means that most of the genes in this module contribute to heat tolerance by RNA modification, translation, DNA replication, and recombinational repair (Fig. S8c). Additionally, KEGG analysis of ‘268’MEsalmon indicated that the DEGs were enriched in ‘ribosome and ribosome biogenesis in eukaryotes’ pathways (Fig. S8d).

In ‘334’MEMidnightblue, GO analysis identified ‘response to heat’ and ‘protein folding’ as the most significantly enriched biological processes, and KEGG analysis identified ‘protein processing in endoplasmic reticulum’ as the most significantly enriched metabolic pathway. Protein folding may be the key biological function for plants to resist the damage caused by high temperature (Fig. 6). For ‘334’MELightcyan and ‘334’MEblue, GO analysis indicated that ‘regulation of protein serine/threonine phosphatase activity’, ‘response to nitrate’, and ‘iron ion homeostasis’

were the most significantly enriched biological processes upon exposure of *B. rapa* ‘334’ to heat stress for 8 days (Figs. 7 and 8). Notably, KEGG analysis identified ‘carbon metabolism’, ‘nitrogen metabolism’, and ‘histidine metabolism’ as the most significantly enriched metabolic pathways. The GO and KEGG analysis of ‘334’MEgreenyellow indicated that ‘glucosinolate biosynthetic process’ and ‘2-oxocarboxylic acid metabolism’ were the most significantly enriched biological processes and metabolic pathways (Fig. 9). GO analysis identified ‘flavonoid glucuronidation’ and ‘response to toxic substance’ as the most important biological processes, and KEGG analysis indicated ‘sulfur metabolism’ and ‘fatty acid degradation’ as the most significant pathways in ‘334’MEDarkgreen, suggesting that they were engaged in diverse metabolic pathways and toxic substance processing during the 4-day recovery under 25 °C (Fig. S9).

### Hub genes related to the heat stress response in the two *B. rapa* accessions

To obtain further details about the expression patterns of key individual genes, we assigned hub genes in each identified module. The top 20 genes, which had the largest hubness with others, were rebadged as ‘hub genes’ and represented the modules (Figs. 5, 6, 7, 8 and 9 and S9). Further information on the hub genes is provided in the Table S5, S6.

‘268’MEcyan and MEsalmon were the modules most tightly associated with heat stress in ‘268’. Eleven hub genes of ‘268’MEcyan were identified in the ‘268’MEcyan module, including eight encoding proteins, a cytochrome P450 76C4, and MADS-box transcription factor PHERES 2. Notably, *NAC055*, a member of the NAC domain-containing protein family, plays a key role in diverse biological processes such as the water deprivation response, jasmonic acid-mediated signaling pathway, response to hydrogen peroxide, and positive regulation of leaf senescence. *PPD*, as a pheophorbidease, was enriched in the porphyrin and chlorophyll metabolism pathways and is involved in leaf senescence and chlorophyll a catabolic process. Furthermore, NAD(H) kinase 1 (*NADK1*) was associated with the NADP biosynthetic process and nicotinate and nicotinamide metabolism. *DJIA*, protein DJ-1 homolog A, is involved in biological processes such as cellular response to hydrogen peroxide (GO:0,070,301) and positive regulation of cellular response to oxidative stress (GO:1,900,409). Serine carboxypeptidase-like 11 (*SCPL11*), cytochrome P450 76C4 (*CYP76C4*), and berberine bridge enzyme-like 7 (*FOX5*) were enriched in the oxidation–reduction process. *PSY1* was annotated in intracellular signal transduction and *PHE2*, a member of MADS-box transcription factor PHERES 2, positively regulates the transcription from RNA polymerase II

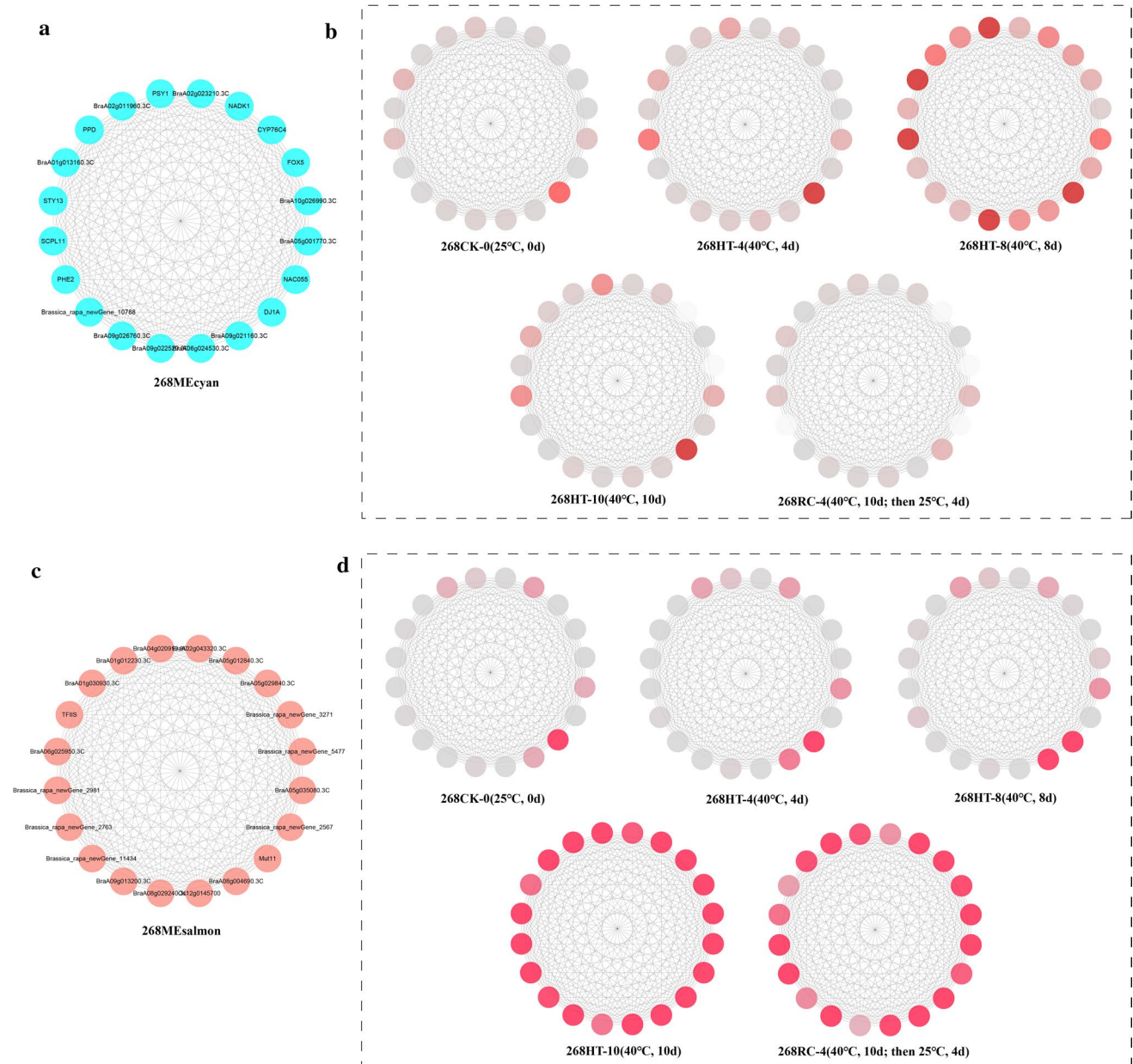


**Fig. 5** Hub genes and expression profiles of heat stress-related key modules in ‘268’. **a** Co-expression gene networks with the greatest hubness in ‘268’ MEcyan. The top 20 genes are defined as hub genes and shown in the nodes with their gene name. Nodes are represented by dots coated with module colors. **b** Mean expression profiles of the hub genes in different heat stress treatments of ‘CK-0’, ‘HT-4’, ‘HT-8’, ‘HT-10’, ‘RC-4’ in ‘268’ samples. The locations of each gene correspond to (a). The mean expression level of the hub genes is indicated by log<sub>2</sub> FPKM values and displayed by the depth of the color. The darker the red color, the higher the expression level. **c** Co-expression

gene networks with the greatest hubness in ‘268’ MEsalmon. The top 20 genes are defined as hub genes and shown in the nodes with their gene name. Nodes are represented by dots coated with module colors. **d** Mean expression profiles of the hub genes in different heat stress treatments of ‘CK-0’, ‘HT-4’, ‘HT-8’, ‘HT-10’, ‘RC-4’ in ‘268’ samples. The locations of each gene correspond to (c). The mean expression level of the hub genes is indicated by log<sub>2</sub> FPKM values and displayed by the depth of the color. The darker the red color, the higher the expression level

promoter. For ‘268’ MEsalmon, only two of the 20 genes were annotated. One is transcription elongation factor *TFIIS*, and the other is the protein *Mut11*. *TFIIS* belongs to DNA-templated, and *Mut11* belongs to nucleotide binding. We observed that in all the detected modules, the hub

genes in ‘268’ MEcyan and MEsalmon were particularly highly expressed under long-term heat stress compared to the 4-day heat stress and recovery (Fig. 5). In our results, most of the hub genes were related to heat stress, oxidative stress, and leaf senescence.

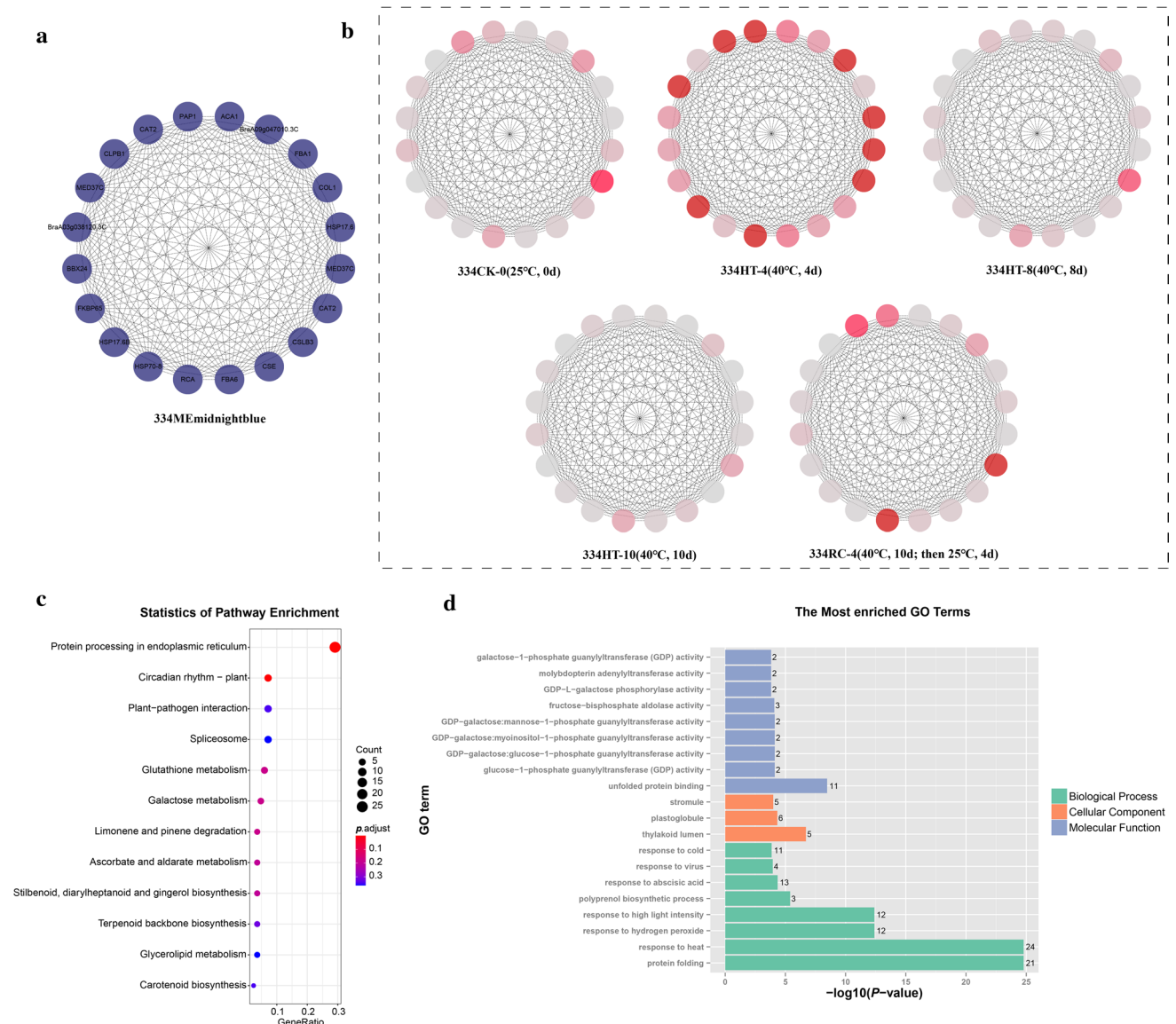


**Fig. 6** Hub genes and expression profiles in ‘334’ MEMidnightblue closely related to ‘HT-4’ in *B. rapa* ‘334’. **a** Co-expression gene networks with the greatest hubness in ‘334’ MEMidnightblue. The top 20 genes are defined as hub genes and shown in the nodes with their gene name. Nodes are represented by dots coated with module colors. **b** Mean expression profiles of the hub genes in different heat stress treatments of ‘CK-0’, ‘HT-4’, ‘HT-8’, ‘HT-10’, ‘RC-4’ in ‘334’ samples. The locations of each gene correspond to (a). The mean expression level of the hub genes is indicated by log<sub>2</sub> FPKM values and displayed by the depth of the color. The darker the red color, the higher the expression level. **c** KEGG enrichment analysis of DEGs belonging to the MEMidnightblue under 4 days of heat stress in *B.*

*rapa* ‘334’. The *p.adjust* is the multiple hypothesis test-corrected *P* value and it ranges from [0–1]. The closer that number is to 0, the more significant the enrichment is. The GeneRatio refers to the ratio of all genes among the DEGs located in a pathway to the total number of DEGs. The greater the GeneRatio, the greater the degree of enrichment is. **d** GO enrichment analysis of DEGs belonging to the MEMidnightblue under 4 days of heat stress in *B. rapa* ‘334’. GO enrichment analysis was performed for the three main categories: green represents biological process, orange represents cellular component, and purple represents molecular function. The X coordinates in the diagram are GO terms, and the Y coordinates are  $-\log_{10}(P\text{-value})$

In ‘334’ MEMidnightblue, six hub genes (*MED37C*, *HSP17.6*, *HSP17.6B*, *HSP70-8*, *CLPB1*), which act as chaperones, were enriched in protein processing in endoplasmic reticulum pathways, indicating that the transferase regulatory network may play a pivotal role in the regulation of heat stress. In addition, there were three genes that

responded to different hormones; for example, *PAP1*, *RCA*, and *FBA6* were related to ABA, jasmonic acid (JA), and cytokinin, respectively. These genes were highly expressed in ‘334’ MEMidnightblue, suggesting that protein processing in the endoplasmic reticulum and plant hormone signal

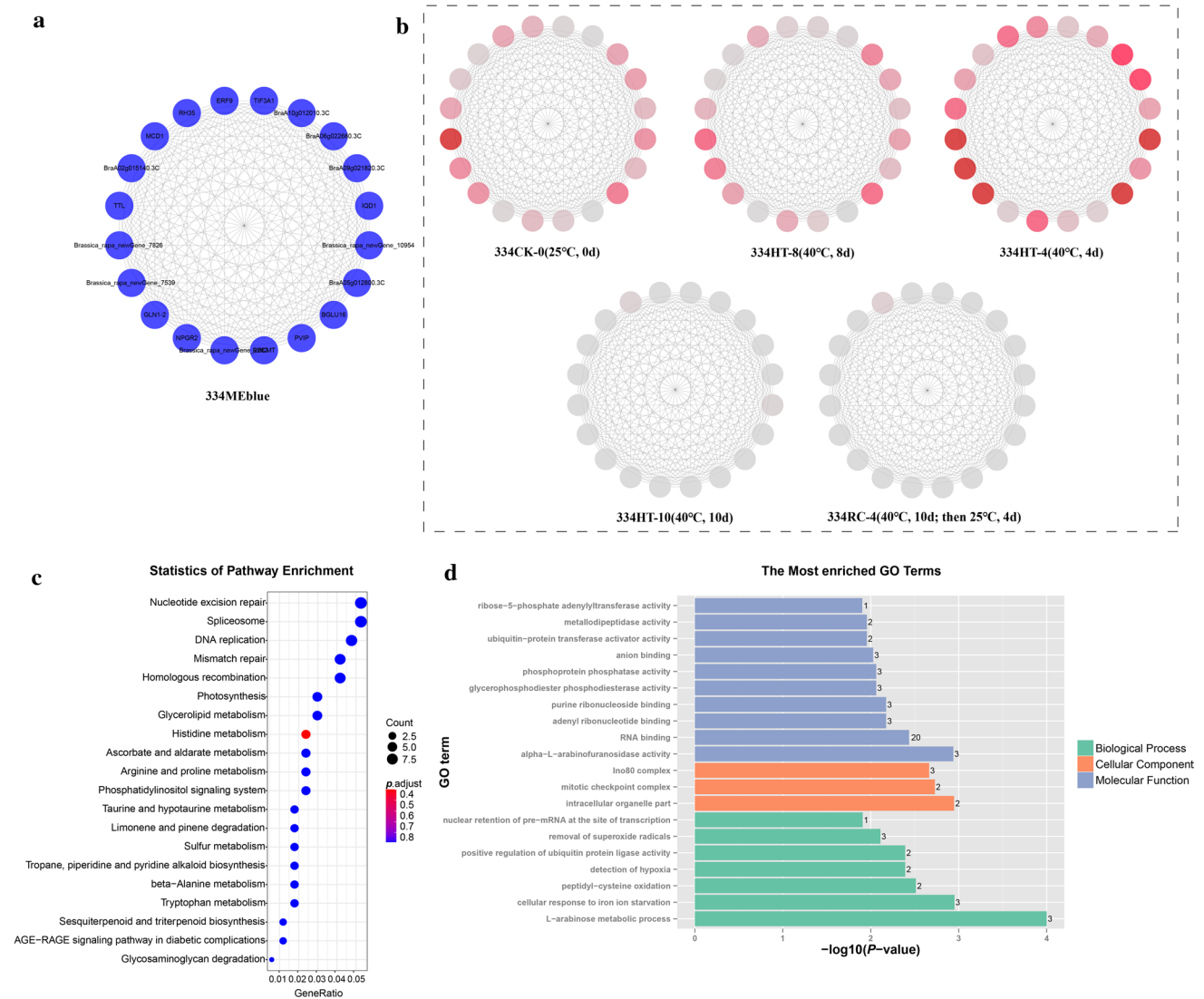


**Fig. 7** Hub genes and expression profiles in ‘334’MEblue closely related to ‘HT-8’ in *B. rapa* ‘334’. **a** Co-expression gene networks with the greatest hubness in ‘334’MEblue. The top 20 genes are defined as hub genes and shown in the nodes with their gene name. Nodes are represented by dots coated with module colors. **b** Mean expression profiles of the hub genes in different heat stress treatments of ‘CK-0’, ‘HT-4’, ‘HT-8’, ‘HT-10’, ‘RC-4’ in ‘334’ samples. The locations of each gene correspond to **a**. The mean expression level of the hub genes is indicated by log<sub>2</sub> FPKM values and displayed by the depth of the color. The darker the red color, the higher the expression level. **c** KEGG enrichment analysis of DEGs belonging to the MEblue under 8 days of heat stress in *B. rapa* ‘334’. The *p*.adjust is

the multiple hypothesis test-corrected *P* value and it ranges from 0 to 1. The closer that number is to 0, the more significant the enrichment is. The GeneRatio refers to the ratio of all genes among the DEGs located in a pathway to the total number of DEGs. The greater the GeneRatio, the greater the degree of enrichment is. **d** GO enrichment analysis of DEGs belonging to the MEblue under 8 days of heat stress in *B. rapa* ‘334’. GO enrichment analysis was performed for the three main categories: green represents biological process, orange represents cellular component, and purple represents molecular function. The X coordinates in the diagram are GO terms, and the Y coordinates are  $-\log_{10}(P\text{-value})$

transduction pathways could help *B. rapa* resist stress and regulate leaf senescence.

‘334’MEblue and MELightcyan were both tightly associated with 8 days of heat stress in *B. rapa* ‘334’. In ‘334’MEblue, the top 20 genes encode transcription factors and other proteins, including ethylene-responsive transcription factor 9, glutamine synthetase cytosolic isozyme

1–2, NPGR2, MULTIPLE CHLOROPLAST DIVISION SITE 1, ribulose-1,5 bisphosphate carboxylase/oxygenase large subunit N-methyltransferase, uric acid degradation bifunctional protein TTL, beta-glucosidase 16, OBERON-like protein, DEAD-box ATP-dependent RNA helicase, and IQ-DOMAIN 1. In particular, *ERF9*, ethylene-responsive transcription factor 9, is involved in the ethylene-activated

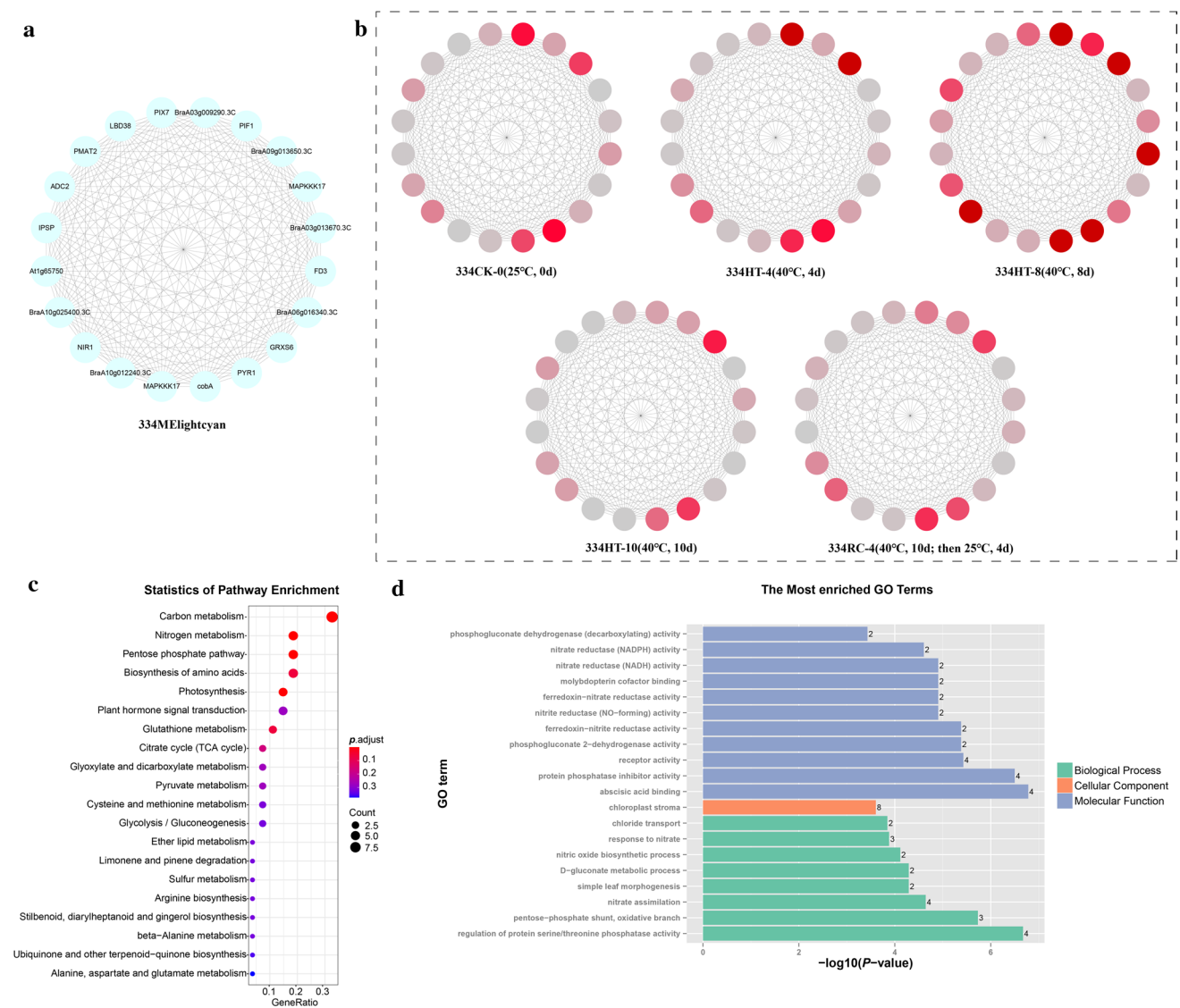


**Fig. 8** Hub genes and expression profiles in ‘334’MELightcyan closely related to ‘HT-8’ in *B. rapa* ‘334’. **a** Co-expression gene networks with the greatest hubness in ‘334’MELightcyan. The top 20 genes are defined as hub genes and shown in the nodes with their gene name. Nodes are represented by dots coated with module colors. **b** Mean expression profiles of the hub genes in different heat stress treatments of ‘CK-0’, ‘HT-4’, ‘HT-8’, ‘HT-10’, ‘RC-4’ in ‘334’ samples. The locations of each gene correspond to **a**. The mean expression level of the hub genes is indicated by  $\log_2$  FPKM values and displayed by the depth of the color. The darker the red color, the higher the expression level. **c** KEGG enrichment analysis of DEGs belonging to the MELightcyan under 8 days of heat stress in *B. rapa* ‘334’.

signaling pathway. *BGLU16*, beta-glucosidase 16, was enriched in carbohydrate metabolic process and starch and sucrose metabolism. Similarly, in ‘334’MELightcyan, *IPSP*, which encodes metal-independent phosphoserine phosphatase, is involved in various biological process (i.e., starch biosynthetic, glucose 1-phosphate metabolic, galactose catabolic) and metabolic pathways (i.e., gluconeogenesis,

The  $p$ .adjust is the multiple hypothesis test-corrected  $P$  value and it ranges from 0 to 1. The closer that number is to 0, the more significant the enrichment is. The GeneRatio refers to the ratio of all genes among the DEGs located in a pathway to the total number of DEGs. The greater the GeneRatio, the greater the degree of enrichment is. **d** GO enrichment analysis of DEGs belonging to the MELightcyan under 8 days of heat stress in *B. rapa* ‘334’. GO enrichment analysis was performed for the three main categories: green represents biological process, orange represents cellular component, and purple represents molecular function. The X coordinates in the diagram are GO terms, and the Y coordinates are  $-\log_{10}(P\text{-value})$

glycine, serine and threonine metabolism, carbon metabolism, and biosynthesis of amino acids). The ABA receptor *PYR1* participates in ABA-activated signaling and plant hormone signal transduction pathways. The transcription factor *PIF1* was enriched in gibberellic acid-mediated signaling pathway and chlorophyll biosynthetic processes. *ADC2*, as arginine decarboxylase 2, responds to salt stress, ABA,

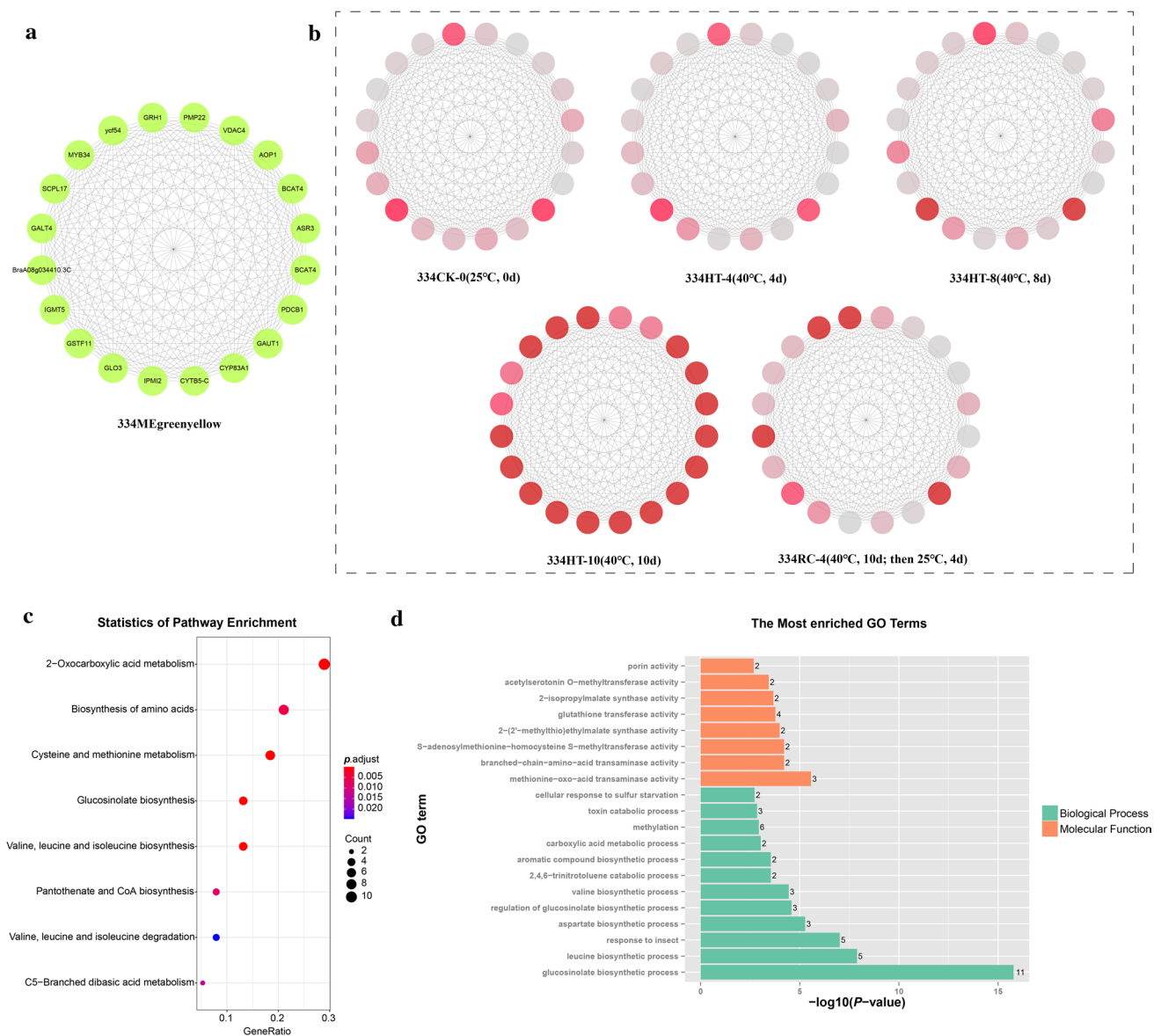


**Fig. 9** Hub genes and expression profiles in ‘334’MEgreenyellow closely related to ‘HT-10’ in *B. rapa* ‘334’. **a** Co-expression gene networks with the greatest hubness in ‘334’MEgreenyellow. The top 20 genes are defined as hub genes and shown in the nodes with their gene name. Nodes are represented by dots coated with module colors. **b** Mean expression profiles of the hub genes in different heat stress treatments of ‘CK-0’, ‘HT-4’, ‘HT-8’, ‘HT-10’, ‘RC-4’ in ‘334’ samples. The locations of each gene correspond to **a**. The mean expression level of the hub genes is indicated by log<sub>2</sub> FPKM values and displayed by the depth of the color. The darker the red color, the higher the expression level. **c** KEGG enrichment analysis of DEGs belonging to the MEgreenyellow under 10 days of heat stress in *B.*

*rapa* ‘334’. The *p.adjust* is the multiple hypothesis test-corrected *P* value and it ranges from 0 to 1. The closer that number is to 0, the more significant the enrichment is. The GeneRatio refers to the ratio of all genes among the DEGs located in a pathway to the total number of DEGs. The greater the GeneRatio, the greater the degree of enrichment is. **d** GO enrichment analysis of DEGs belonging to the MEgreenyellow under ten days of heat stress in *B. rapa* ‘334’. GO enrichment analysis was performed for the three main categories: green represents biological process, orange represents cellular component, and purple represents molecular function. The X coordinates in the diagram are GO terms, and the Y coordinates are  $-\log_{10}(P\text{-value})$

JA, and karrikins. Furthermore, monothiol glutaredoxin-S6 (*GRXS6*), uroporphyrinogen-III C-methyltransferase (*cobA*), and ferredoxin-nitrite reductase (*NIR1*) all contribute to oxidation–reduction process. Mitogen-activated protein kinase kinase kinase 17 (*MAPKKK17*) and probable

serine/threonine-protein kinase (*PIX7*), both signal transducers that act downstream of receptors with serine/threonine kinase activity, participate in protein autophosphorylation process. These hub genes, which mainly encode various proteins involved in complex plant hormone-mediated

signaling pathways exhibited the highest expression levels in ‘334’MEblue and ‘334’MElightcyan, showing that they were largely responsible for heat adaptation and tolerance.

In ‘334’MEgreenyellow, *GAUT1* encoding polygalacturonate 4- $\alpha$ -galacturonosyltransferase function in the pectin biosynthetic process, cell wall organization, and amino sugar and nucleotide sugar metabolism pathways. *VDAC4*, encoding mitochondrial outer membrane protein porin 4, is involved in the regulation of anion transmembrane transport and growth. *BCAT4*, a methionine aminotransferase, and *IPMI2*, 3-isopropylmalate dehydratase small subunit 1, both participate in glucosinolate biosynthetic process in response to stress. *GALT4*, encoding hydroxyproline *O*-galactosyltransferase *GALT4*, is engaged in arabinogalactan protein metabolic process, while *GRH1*, encoding GRR1-like protein 1, is associated with response to auxin, defense response, protein ubiquitination, and developmental growth. Interestingly, there were four hub genes (i.e., *GLO3*, *CYP83A1*, *AOPI1*, and *CYTB5-C*) involved in oxidation–reduction process. The discovery of these key genes indicates that these plants mainly resist heat stress through the oxidation–reduction processes and the toxin decomposition processes in the later stage of long-term heat stress.

‘334’MEdarkgreen was the only module correlated with ‘RC-4’ between the two genotypes of *B. rapa*. One hub gene, named *DJIA*, plays a role in the cellular response to hydrogen peroxide and positively regulated the cellular response to oxidative stress. *CPL1* and *VAL1* are enriched in the ABA-activated signaling pathway, while *AAE3* responds to cytokinin. Furthermore, *NAC102* is involved in the hypoxia response, while the other remaining genes are associated with molecular functions, such as the regulation of transcription, DNA-templated, RNA polymerase, and transport. The expression levels of all the hub genes were significantly changed at the recovery stage compared to each time point under heat stress, demonstrating that the genes were all responsive to recovery after long-term heat stress.

### Verification of hub genes related to the heat stress response by qRT-PCR

A random selection of 10 hub genes related to the heat stress response were verified for qRT-PCR analysis, including four plant hormone signal transduction genes (*SPK2E*, *ATHB-7*, *MAPKKK18*, and *ABI2*), four protein processing in endoplasmic reticulum responses (HSPs *HSP70-17*, *HSP90-6*, *HSP17.6*, and heat stress transcription factor *HSFA2*), and two autophagy (i.e., *ATG8E* and *ATG8A*) genes (Fig. 10; Table S7). Of these genes, with the increasing days of heat stress, the relative expression levels of these three genes (*SPK2E*, *ATHB-7*, and *MAPKKK18*) in *B. rapa* ‘268’ were also increased, then slightly decreased at the ‘RC-4’ stage. However, no obvious expression pattern was observed in

*B. rapa* ‘334’. Besides, four genes (*HSP70-17*, *HSP90-6*, *HSP17.6*, and *HSFA2*) in two *B. rapa* accession reached a peak of expression at the ‘HT-4’ stage and *HSP17.6* remained a higher expression level during heat stress. The expression of *ATG8E* and *ATG8A* reached the highest expression level in *B. rapa* ‘268’ at the ‘HT-8’ stage while they reached the highest expression level in *B. rapa* ‘334’ at the ‘RC-4’ stage. These results suggested that these hub genes may be potential candidates for further analyses of the response to long-term heat stress. In addition, the expression patterns of the RNA-Seq and RT-qPCR analyses were highly consistent, thus confirming the validity of the RNA-Seq results.

## Discussion

### Heat stress response co-expression networks were constructed from two heat *B. rapa* accessions with differing heat resistance using the WGCNA method

Heat stress presents a major obstacle to the growth and development of *B. rapa*, causing loosening of the leafy head and declines in yield and quality (Sato et al. 2002). To our knowledge, the thermotolerance mechanisms of *B. rapa* have not been elucidated and no report exists on the gene interaction network of *B. rapa* under heat stress treatments of different durations. Currently, combination of the WGCNA method and RNA-Seq data has been used to explore the genes and key factors related to the traits (Amrine et al. 2015; Hopper et al. 2016; Kost et al. 2017; Tan et al. 2017; Lin et al. 2019; Wu et al. 2020). Therefore, in this study, we aimed to elucidate the underlying mechanism and offer a novel perspective on this heat-responsive core transcriptome by using the WGCNA method. Based on the RNA-Seq data and morphological indicators of 27 samples for each *B. rapa* accession, we confirmed that ‘268’ and ‘334’ exhibited differing responses to heat stress under high-temperature treatment. First, a comparative analysis of the transcriptome of five treatments under heat stress exposure identified the DEGs unique to each treatment stage. We then used the DEGs identified in the two accessions as input datasets for the WGCNA analysis. This confirmed that DEG analysis and WGCNA are complementary. Moreover, the results showed that the modules identified here are biologically reasonable.

In WGCNA, gene modules with high correlations with accessions can be selected from expressed genes to more specifically assess the expression of genes related to specific traits (Tan et al. 2017; Xie et al. 2019). WGCNA analysis was based on the premise that genes in the same modules with similar expression patterns tend to be functionally relevant (Eisen et al. 1998; Luo et al. 2019; Takehisa and Sato



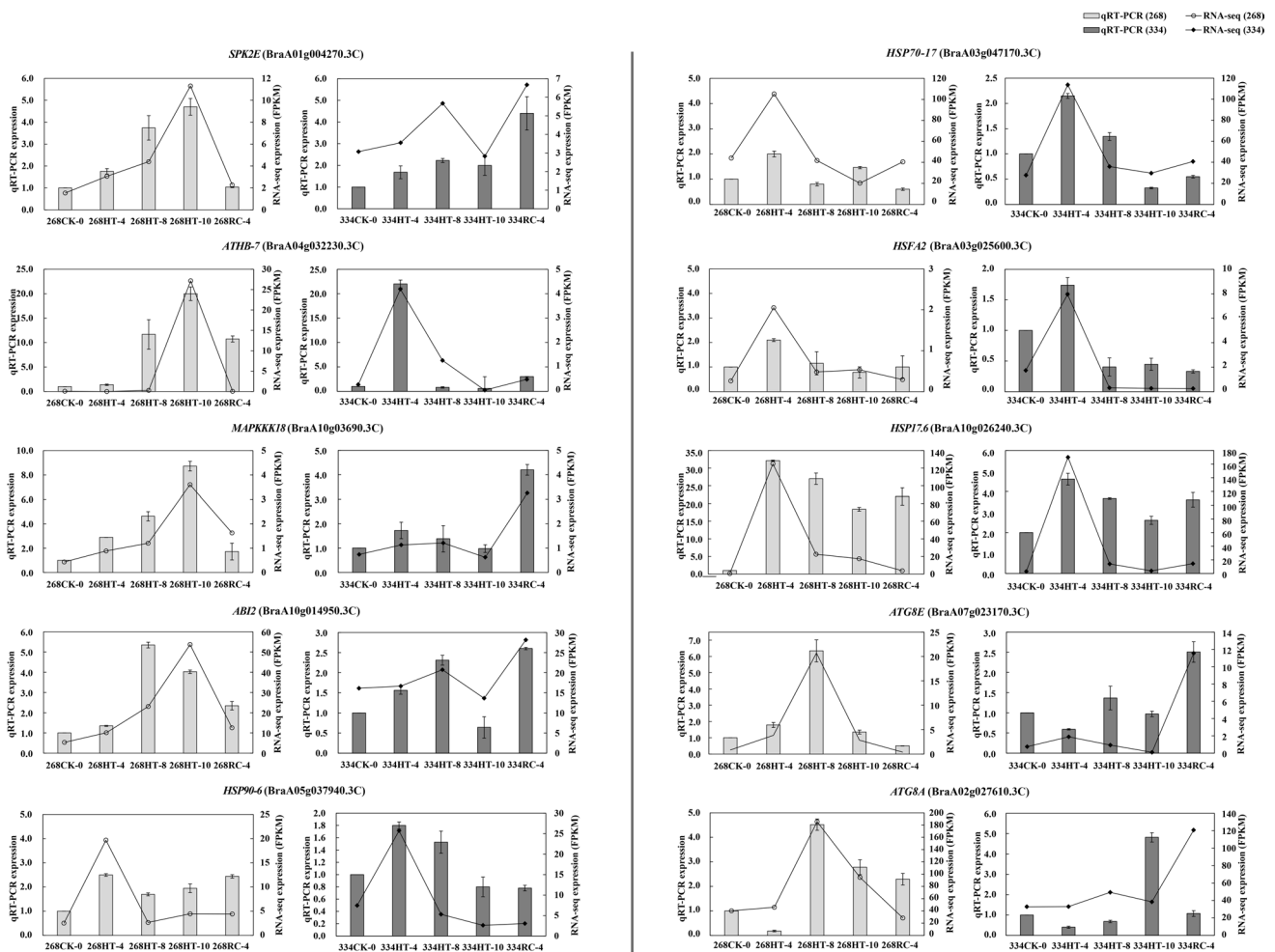


**Fig. 10** The qRT-PCR verification of ten hub genes. The expression analysis of these genes in different heat stress treatments (‘CK-0’, ‘HT-4’, ‘HT-8’, ‘HT-10’, and ‘RC-4’) is shown in two *B. rapa* accessions. The light gray graph indicates the hub gene expression in heat-resistant plant ‘268’ whereas the dark gray graph indicates the hub

gene expression in heat-sensitive plant ‘334’. Bar and line graphs represent the qRT-PCR and RNA-Seq data, respectively. Data are presented as the mean ± standard error (SE). Error bars are based on the mean of three technical replicates

2019). Using the WGCNA gene co-expression network, we systematically analyzed the responses of the *B. rapa* accessions with differing heat tolerance to different heat stress treatment durations at the transcriptome level. For the first time, the modules closely correlated with heat stress in different *B. rapa* accessions were identified, and two gene co-expression networks of DEGs in the two *B. rapa* accessions under different heat-stress treatments were constructed. Based on the gene modules with known biological function predictions, the heat tolerance characteristics of two *B. rapa* accessions under heat stress were analyzed and determined. We then constructed a visual network for each module gene and found the top 20 hub genes with the highest correlation with these modules (Figs. 5, 6, 7, 8 and 9). We discovered that these hub genes exhibited a high degree of connectivity with other key genes. In the gene network, we found that hub genes were mainly enriched in some pivotal transcription

factors, hormones, protein-like carrier proteins, and DNA binding proteins. Interestingly, we found that the genes associated with plant hormone signal transduction pathways and protein processing in endoplasmic reticulum were strongly enhanced under heat stress in *B. rapa*. Changes in the level of expression of core genes indicates that many other genes must also change. We also inferred that these core genes differed in their expression patterns before and after heat stress among the accessions. The different expression patterns may lead to the difference in the response of *B. rapa* to heat stress.

### Difference between long-term heat stress and a short transient heat-shock response

Previous studies have concentrated on the impacts of short-term heat stress or heat shock in plants. For example, the

expression of small HSPs was highly induced, and high-molecular weight HSPs exhibited constitutively high expression, when *B. rapa* was incubated at 45 °C for 0.5, 1, 2, 3, or 4 h (Singh et al. 2019). In tall fescue (*Festuca arundinacea* Schreb.), many genes encoding HSFs, HSPs, FKBP, and calcium and phytohormone signaling were activated by short-term heat stress, while under long-term heat stress, genes involved in chlorophyll catabolism, phytohormone synthesis/degradation, and NAC transcription factors (TFs) were significantly expressed and photosynthesis-related genes were suppressed (Qian et al. 2020). In this study, we focused on long-term heat stress in *B. rapa* and speculated that the response mechanism of short-term heat stress differed from that of long-term heat stress. We observed that in heat-resistant *B. rapa*, the autophagy pathway, glutathione metabolism, and ribosome biogenesis in eukaryotes were significantly up-regulated, while photosynthesis was down-regulated. After a long period of heat stress, the photosynthetic organs of *B. rapa* can become damaged, after which their life activities mainly focused on clearing damaged cells and various metabolisms to maintain their own energy balance. Additionally, our findings that the autophagy-related genes might have been induced by persistent heat stress and remained high during recovery also confirmed the above inference. For the heat-sensitive *B. rapa*, long-term high-temperature stress caused significant changes in the expression of certain functional genes linked to protein processing in the endoplasmic reticulum and plant hormone signal transduction pathways. Since HSPs have been reported to be more expressed under short-term heat stress (Singh et al. 2019; Qian et al. 2020), it appears that in our study only a few DEGs were annotated as HSPs and functioned in long-term heat stress. This may be that short-term stress can stimulate the expression of HSPs, and HSPs detected after long-term heat stress mainly function as molecular chaperones in autophagy and protein processing in the endoplasmic reticulum to help *B. rapa* adapt to heat stress.

### Changes in the HSP and HSF family genes in response to heat

We discovered that protein processing in the endoplasmic reticulum pathway played a key role in the heat-sensitive line '334'. There were 19 genes encoding HSPs and two genes encoding *HSPA2* and *HSPB2A* in the '334' MEMidnightblue module. Most of these DEGs belonged to the HSP20, 70, and 90 families. In particular, several genes, including *HSP17.6*, *HSP17.6B*, *HSP70-8*, *MED37C*, and *CLPBI*, which are involved in the response to protein processing in the endoplasmic reticulum, were identified as the hub genes of the '334' MEMidnightblue module. Previous research indicated that thermotolerance in *Arabidopsis* can be divided into acquired thermotolerance and basal

thermotolerance (Liu et al. 2015). Plants can gain heat tolerance through exposure to moderate heat stress. This acquired thermotolerance enables plants to tolerate heat stress that is fatal to native plants. Interestingly, plants will actively maintain this heat stress memory for several days. It was reported that HSFs and HSPs have a role in heat stress and acquired thermotolerance in plants (Liu et al. 2015). In particular, the heat shock transcription factor *HSPA2*, as a major heat stress factor, functions in the heat stress memory and induces the expression of HSPs, but is only expressed in stressed plants (Scharf et al. 2012). Moreover, it is regarded as the most strongly induced protein in tomato (*Solanum lycopersicum* L.), *Arabidopsis*, and rice and accumulates to high levels in plants exposed to heat shock for a long time or repeated heat shock and recovery cycles (Scharf et al. 2012). The overexpression of *HSPA2* is sufficient to enhance the comprehensive resistance to heat, salt, osmotic stress, hypoxia, high light, and oxidative stress (Jacob et al. 2017). *CaHsfB2a* of pepper, which is involved in a cascade with *CaWRKY6* and *CaWRKY40*, positively regulates plant tolerance to high-temperature high-humidity conditions (Ashraf et al. 2018). Our present results are consistent with others in *B. rapa*. When suffering from heat stress at 40 °C for 4 days, *HSPA2* displayed high expression in both the heat-resistant '268' and heat-sensitive '334'. Compared with the heat-resistant '268', heat-sensitive '334' exhibited higher expression in 'HT-4'.

Upon exposure to high temperature, newly synthesized proteins in plants would become misfolded, while existing proteins would be denatured. HSPs, as chaperones, are well established as being vital in biotic and abiotic stress tolerance, as they can maintain protein functional conformation and prevent non-native proteins from aggregation (Qu et al. 2013). The expression of HSPs is mediated by HSFs. Several studies have observed that many HSPs, such as HSP101, HSP90, HSP 70, and low-molecular-weight HSPs, change under heat stress. The present study further strengthens the evidence that *HSP101* participates in thermo-tolerance in maize, *Arabidopsis*, and cotton (*Gossypium hirsutum* L.) (Queitsch et al. 2000; Nieto-Sotelo et al. 2002; Saleem et al. 2021). Wang et al. (2016) found that *HSP70*, *HSP101*, and *HSPB27* were induced after heat stress in *B. rapa*. *HSP70* participates in the feedback control of heat stress and negatively regulates the heat stress response. *HSP70s* have been observed under heat stress in many vegetables, such as pepper, potato (*Solanum tuberosum* L.), cabbage, and tomato (Guo et al. 2016; Lee et al. 2018; Liu et al. 2018; Zhang et al. 2018b). Under heat stress, the expression level of *HSP90* was also high, and *HSP90.1* has been reported in rice and *Arabidopsis* (Hu et al. 2009; Prasad et al. 2010), and all classes of HSP90 (A, B, and C) have been detected in soybeans (Xu et al. 2013). Low-molecular-weight HSPs (i.e., - 18.1 and - 17.9) accumulated in pea under storage

at 42 °C for 4 h (Avelange-Macherel et al. 2015). The correlation of small HSPs with HSP100, HSP70, and HSP60 in a previous study suggests their role as participants in disaggregation and protein folding (Wang et al. 2014). In our study, three hub genes encoding *HSP17.6*, *HSP17.6B*, and *HSP70-8* were identified in the '334'MEmidnightblue module. Moreover, hub gene *CLPB1*, named *AtHsp101* in *Arabidopsis*, is one of the best-studied proteins from this family and plays an essential role in adaptation to heat tolerance (Hong and Vierling 2000; Lee et al. 2007). We speculate that HSPs and other proteins, as chaperones, play a key role in heat stress tolerance in *B. rapa*.

### Photosynthesis under high temperature behaves differently in two *B. rapa* accessions with different heat sensitivities

Previous studies have revealed that metabolic processes, such as photosynthesis, chlorophyll content, carbon fixation, and sucrose metabolism, are inhibited by heat stress, while respiration is increased (Kaushal et al. 2013). Thus, photosynthetic efficiency would be suppressed upon exposure to heat stress (Julius et al. 2017; Saleem et al. 2021). In the present study, KEGG analysis indicated that the DEGs identified at the stage 'CK-8 vs. HT-8' and 'CK-10 vs. HT-10' in *B. rapa* '268' were down-regulated in the photosynthesis pathway, indicating that the photosynthetic apparatus was damaged after long-term heat stress. However, in *B. rapa* '334', DEGs unique to the 'CK-10 vs. HT-10' stage were significantly up-regulated. Thus, we inferred that plants attempted to reduce the damage caused by high temperature by removing reactive oxygen species (ROS) and maintaining steady photosynthesis. Photosynthesis behaved differently in the two *B. rapa* accessions under high-temperature stress, which may be one of the key factors causing the differences in the heat resistance of the two materials. Additional discussion and experiments are needed to verify this inference.

### Complex hormone network regulation affects heat tolerance

Phytohormones in plants also have a profound impact on the response to various abiotic stresses. Major hormones contained in plants include auxins, ABA, cytokinins, ethylene (ET), gibberellins (GA), salicylic acid (SA), jasmonates (JA), and brassinosteroids (BR). Among these, ABA, SA, JA, and ET have non-substitute advantages in mediating the plant defense response against pathogens and abiotic stresses (Bari and Jones 2008; Verma et al. 2016). ABA, which is an isoprenoid (Nambara and Marion-Poll 2005), is one of the most important phytohormones involved in plant growth, development, and adaptation to various stress conditions (Merlot et al. 2001). In our study, *PAP1* in '334'MEmidnightblue,

*PYR1* and *ADC2* in '334'MElightcyan, and *CPL1* and *VAL1* in '334'MEdarkgreen were identified as hub genes and were enriched in ABA-activated signaling pathway. In *Arabidopsis*, interactions between *PYR/PYL/RCARs* and *PP2C* can be promoted by ABA, such that *SnRK2* phosphorylates downstream components required to regulate gene expression or gated ion channels (Park and Kim 2017). *CPL1* is a gene sensitive to biotic stress that functions in abiotic stress signaling (Thatcher et al. 2018). *ADC2* belongs to the polyamine (PA) biosynthetic pathway and is regulated at the transcriptional level during abiotic stresses (Perez-Amador 2002; Sagor et al. 2012). Upon exposure to high temperature in *Arabidopsis*, the expression of *ADC2* is up-regulated (Sagor et al. 2012). Additionally, *ADC2* can regulate the ABA and JA signaling pathways (Perez-Amador 2002). JAs, which are regarded as regulators and defenders of plant growth and signals, function in various abiotic and biotic stress responses, as well as in leaf senescence (Wasternack 2007; Reinbothe et al. 2009; Shan et al. 2011). *RCA*, which encodes ribulose-1,5-bisphosphate carboxylase/oxygenase and is located in the stroma of chloroplasts, is the principal enzyme that fixes CO<sub>2</sub> (Shan et al. 2011). Wijewardene et al. recently demonstrated that overexpression of *RCA* could maintain photosynthesis at higher temperatures, contributing to higher heat tolerance in transgenic plants (Wijewardene et al. 2020). We identified *RCA* as one of the hub genes in the '334'MEmidnightblue module. In addition, *PIF1*, one of the hub genes of the '334'MElightcyan module, was enriched in ABA biosynthesis and was found to regulate chlorophyll biosynthesis to optimize the greening process in *Arabidopsis* (Moon et al. 2008; Oh et al. 2009). *AAE3*, one of the hub genes of the '334'MEdarkgreen module, was enriched in the response to cytokinin and is involved in oxalate degradation and aluminum tolerance. *GRH1*, one of the hub genes of the '334'MEgreenyellow module, was also enriched in auxin response. *ERF9*, one of the hub genes of the '334'MEblue module, functions in the ET-activated signaling pathway. However, no reports have confirmed whether these genes are related to heat stress. The current study revealed that the expression of these genes increased significantly under heat stress and thus they might also contribute to high-temperature stress resistance. From the foregoing discussion, it is clear that plants utilize elaborate plant hormone signal transduction pathways in the response to long-term high temperatures and heat stress, although the roles of these hub genes in heat stress have not been demonstrated. Additional experiments are needed to determine their roles and downstream pathways in thermotolerance.

### Autophagy-related genes might protect *B. rapa* against heat stress

The autophagy pathway is another means by which plants protect themselves against heat stress. At the cellular level,

autophagy can remove non-functional proteins or damaged cellular components to maintain energy balance (Pietrocola et al. 2013). Several studies have reported that autophagy has a vital role in the heat stress response in plants. For example, autophagy may reduce the severe damage caused by the excess accumulation of aggregated proteins and decreased heat tolerance upon exposure to heat stress in tomato and *Arabidopsis* (Zhou et al. 2013, 2014). It was reported that autophagy is induced by thermoprime and remains high in *Arabidopsis* during the recovery stage (Sedaghatmehr et al. 2019). Our research also confirmed the above finding. In ‘CK-8 vs. HT-8’, KEGG analysis indicated DEGs significantly up-regulated in the autophagy pathway. Twelve autophagy-related genes were annotated in ‘268’ MEcyan closely related to ‘HT-10’, while four genes related to ‘RC-4’ were annotated in ‘334’ MEsalmon. These genes exhibited a higher level of expression during the recovery period. Therefore, we propose that these autophagy-related genes could be functionally characterized using reverse genetic experiments. Altogether, additional work, including proteomics, and metabolomics analyses, is clearly needed to further delineate the response to long-term heat stress in *B. rapa* and will contribute to a more detailed description of the dynamics of heat stress adaptation in general.

## Conclusion

We systematically analyzed the differential responses of the transcriptomes of *B. rapa* accessions ‘268’ and ‘334’, which differ in their heat tolerance, to long-term heat stress. Comparative analysis and gene co-expression network analysis of the heat-responsive core transcriptome in two contrasting *B. rapa* accessions revealed the main metabolic pathways, key modules and hub genes involved in long-term heat stress and recovery. Particularly, the autophagy pathway, glutathione metabolism, and ribosome biogenesis in eukaryotes were noticeably up-regulated, whereas photosynthesis was inhibited, in the heat stress response of *B. rapa* ‘268’. For the heat-sensitive *B. rapa* ‘334’, heat stress caused significant changes in the expression of certain functional genes linked to protein processing in the endoplasmic reticulum and plant hormone signal transduction pathways. Several hub genes associated with the HSPs *HSP17.6*, *HSP17.6B*, *HSP70-8*, *CLPB1*, *PAP1*, *PYR1*, *ADC2*, and *GSTF11* were involved in protein processing in the endoplasmic reticulum response, plant hormone signal transduction, and oxidation–reduction processes. Overall, the data provided here reveal a genome-wide transcriptional landscape of the long-term heat stress response in *B. rapa*, which furthers our knowledge of how *B. rapa* responds to long-term heat stress and provides a mechanistic molecular basis for further research into heat stress in *B. rapa* in the future.

**Author contributions statement** SZ and RS conceived and designed the experiments. LY and GL performed the experiments. XS, FL, SZ, and HZ provided support for experimental methods and experimental materials. LY analyzed the data and wrote the manuscript. LG and YD contributed revision of this paper. All authors have read and approved the final manuscript.

**Supplementary Information** The online version contains supplementary material available at <https://doi.org/10.1007/s00425-021-03630-3>.

**Acknowledgements** We thank Prof. Cheng Feng and Dr. Zhang Kang (Institute of Vegetables and Flowers, Chinese Academy of Agricultural Sciences, Beijing, China) for help and advice on transcriptome data analysis. We thank LetPub ([www.letpub.com](http://www.letpub.com)) for its linguistic assistance during the preparation of this manuscript.

**Funding** This work was funded by the National Key Research and Development Program of China (Grant number 2017YFD0101802) and the Agricultural Science and Technology Innovation Program of the Chinese Academy of Agricultural Sciences (CAAS-ASTIP-IVF-CAAS). This work was performed at the Key Laboratory of Biology and Genetic Improvement of Horticultural Crops, Ministry of Agriculture, Beijing, China.

## Declarations

**Conflicts of interest** The authors declare that they have no competing interests.

## References

- Amrine KC, Blanco-Ulate B, Cantu D (2015) Discovery of core biotic stress responsive genes in *Arabidopsis* by weighted gene co-expression network analysis. PLoS ONE 10:e0118731. <https://doi.org/10.1371/journal.pone.0118731>
- Anders S, Huber W (2010) Differential expression analysis for sequence count data. Genome Biol 11:R106. <https://doi.org/10.1186/gb-2010-11-10-r106>
- Ashraf MF, Yang S, Wu R, Wang Y, Hussain A, Noman A, Khan MI, Liu Z, Qiu A, Guan D, He S (2018) *Capsicum annuum* *HsfB2a* positively regulates the response to *Ralstonia solanacearum* infection or high temperature and high humidity forming transcriptional cascade with *CaWRKY6* and *CaWRKY40*. Plant Cell Physiol 59:2608–2623. <https://doi.org/10.1093/pcp/pcy181>
- Avelange-Macherel MH, Payet N, Lalanne D, Neveu M, Tolleter D, Burstin J, Macherel D (2015) Variability within a pea core collection of LEAM and HSP22, two mitochondrial seed proteins involved in stress tolerance. Plant Cell Environ 38:1299–1311. <https://doi.org/10.1111/pce.12480>
- Avin-Wittenberg T (2019) Autophagy and its role in plant abiotic stress management. Plant Cell Environ 42:1045–1053. <https://doi.org/10.1111/pce.13404>
- Awasthi R, Bhandari K, Nayyar H (2015) Temperature stress and redox homeostasis in agricultural crops. Front Environ Sci 3:11. <https://doi.org/10.3389/fenvs.2015.00011>
- Bari R, Jones JDG (2008) Role of plant hormones in plant defence responses. Plant Mol Biol 69:473–488. <https://doi.org/10.1007/s11103-008-9435-0>

- Benjamini Y, Hochberg Y (1995) Controlling the false discovery rate - a practical and powerful approach to multiple testing. *J R Stat Soc* 57:289–300. <https://doi.org/10.2307/2346101>
- Bokszczanin KL, Network SPTIT, C, Fragkostefanakis S, (2013) Perspectives on deciphering mechanisms underlying plant heat stress response and thermotolerance. *Front Plant Sci* 4:315. <https://doi.org/10.3389/fpls.2013.00315>
- Challinor AJ, Watson J, Lobell DB, Howden SM, Smith DR, Chhetri N (2014) A meta-analysis of crop yield under climate change and adaptation. *Nat Clim Chang* 4:287–291. <https://doi.org/10.1038/nclimate2153>
- Cheng F, Liu S, Wu J, Fang L, Sun S, Liu B, Li P, Hua W, Wang X (2011) BRAD, the genetics and genomics database for Brassica plants. *BMC Plant Biol* 11:136. <https://doi.org/10.1186/1471-2229-11-136>
- Chin CH, Chen SH, Wu HH, Ho CW, Ko MT, Lin CY (2014) cytoHubba: identifying hub objects and sub-networks from complex interactome. *BMC Syst Biol* 8(Suppl 4):S11. <https://doi.org/10.1186/1752-0509-8-S4-S11>
- Dai Y, Zhang S, Sun X, Li G, Yuan L, Li F, Zhang H, Zhang S, Chen G, Wang C, Sun R (2020) Comparative transcriptome analysis of gene expression and regulatory characteristics associated with different vernalization periods in *Brassica rapa*. *Genes* (Basel). <https://doi.org/10.3390/genes11040392>
- DeRocher AE, Helm KW, Lauzon LM, Vierling E (1991) Expression of a conserved family of cytoplasmic low molecular weight heat shock proteins during heat stress and recovery. *Plant Physiol* 96:1038–1047. <https://doi.org/10.1104/pp.96.4.1038>
- Dong X, Yi H, Lee J, Nou IS, Han CT, Hur Y (2015) Global gene-expression analysis to identify differentially expressed genes critical for the heat stress response in *Brassica rapa*. *PLoS ONE* 10:e0130451. <https://doi.org/10.1371/journal.pone.0130451>
- Eisen MB, Spellman PT, Brown PO, Botstein D (1998) Cluster analysis and display of genome-wide expression patterns. *Proc Natl Acad Sci USA* 95(25):14863–14868. <https://doi.org/10.1073/pnas.95.25.14863>
- Guo M, Liu JH, Ma X, Zhai YF, Gong ZH, Lu MH (2016) Genome-wide analysis of the Hsp70 family genes in pepper (*Capsicum annuum* L.) and functional identification of CaHsp70-2 involvement in heat stress. *Plant Sci* 252:246–256. <https://doi.org/10.1016/j.plantsci.2016.07.001>
- Han Y, Yong X, Yu J, Cheng T, Wang J, Yang W, Pan H, Zhang Q (2019) Identification of candidate adaxial-abaxial-related genes regulating petal expansion during flower opening in *Rosa chinensis* “Old Blush.” *Front Plant Sci* 10:1098. <https://doi.org/10.3389/fpls.2019.01098>
- Hong S-W, Vierling E (2000) Mutants of *Arabidopsis thaliana* defective in the acquisition of tolerance to high temperature stress. *Proc Natl Acad Sci USA* 97:4392–4397. <https://doi.org/10.1073/pnas.97.8.4392>
- Hopper DW, Ghan R, Schlauch KA, Cramer GR (2016) Transcriptomic network analyses of leaf dehydration responses identify highly connected ABA and ethylene signaling hubs in three grapevine species differing in drought tolerance. *BMC Plant Biol* 16:118. <https://doi.org/10.1186/s12870-016-0804-6>
- Hu W, Hu G, Han B (2009) Genome-wide survey and expression profiling of heat shock proteins and heat shock factors revealed overlapped and stress specific response under abiotic stresses in rice. *Plant Sci* 176:583–590. <https://doi.org/10.1016/j.plantsci.2009.01.016>
- Huang XY, Tao P, Li BY, Wang WH, Yue ZC, Lei JL, Zhong XM (2015) Genome-wide identification, classification, and analysis of heat shock transcription factor family in Chinese cabbage (*Brassica rapa pekinensis*). *Genet Mol Res* 14:2189–2204. <https://doi.org/10.4238/2015.March.27.5>
- Isah T (2019) Stress and defense responses in plant secondary metabolites production. *Biol Res* 52:39. <https://doi.org/10.1186/s40659-019-0246-3>
- Jacob P, Hirt H, Bendahmane A (2017) The heat-shock protein/chaperone network and multiple stress resistance. *Plant Biotechnol J* 15:405–414. <https://doi.org/10.1111/pbi.12659>
- Julius BT, Leach KA, Tran TM, Mertz RA, Braun DM (2017) Sugar transporters in plants: new insights and discoveries. *Plant Cell Physiol* 58:1442–1460. <https://doi.org/10.1093/pcp/pcx090>
- Kaushal N, Awasthi R, Gupta K, Gaur P, Siddique KHM, Nayyar H (2013) Heat-stress-induced reproductive failures in chickpea (*Cicer arietinum*) are associated with impaired sucrose metabolism in leaves and anthers. *Funct Plant Biol* 40:1334–1349. <https://doi.org/10.1071/FP13082>
- Kost MA, Perales HR, Wijeratne S, Wijeratne AJ, Stockinger E, Mercer KL (2017) Differentiated transcriptional signatures in the maize landraces of Chiapas, Mexico. *BMC Genom* 18:707. <https://doi.org/10.1186/s12864-017-4005-y>
- Langfelder P, Horvath S (2008) WGCNA: an R package for weighted correlation network analysis. *BMC Bioinform* 9:559. <https://doi.org/10.1186/1471-2105-9-559>
- Lee U, Rioflorida I, Hong SW, Larkindale J, Waters ER, Vierling E (2007) The *Arabidopsis* ClpB/Hsp100 family of proteins: chaperones for stress and chloroplast development. *Plant J* 49:115–127. <https://doi.org/10.1111/j.1365-3113.2006.02940.x>
- Lee SS, Jung WY, Park HJ, Lee A, Kwon SY, Kim HS, Cho HS (2018) Genome-wide analysis of alternative splicing in an inbred Cabbage (*Brassica oleracea* L.) line “HO” in response to heat stress. *Curr Genom* 19:12–20. <https://doi.org/10.2174/1389202918666170705151901>
- Li H, Liu SS, Yi CY, Wang F, Zhou J, Xia XJ, Shi K, Zhou YH, Yu JQ (2014) Hydrogen peroxide mediates abscisic acid-induced HSP70 accumulation and heat tolerance in grafted cucumber plants. *Plant Cell Environ* 37:2768–2780. <https://doi.org/10.1111/pce.12360>
- Li S, Yu J, Li Y, Zhang H, Bao X, Bian J, Xu C, Wang X, Cai X, Wang Q, Wang P, Guo S, Miao Y, Chen S, Qin Z, Dai S (2019) Heat-responsive proteomics of a heat-sensitive Spinach variety. *Int J Mol Sci* 20:3872. <https://doi.org/10.3390/ijms20163872>
- Lin CW, Fu SF, Liu YJ, Chen CC, Chang CH, Yang YW, Huang HJ (2019) Analysis of ambient temperature-responsive transcriptome in shoot apical meristem of heat-tolerant and heat-sensitive broccoli inbred lines during floral head formation. *BMC Plant Biol* 19:3. <https://doi.org/10.1186/s12870-018-1613-x>
- Liu J, Feng L, Li J, He Z (2015) Genetic and epigenetic control of plant heat responses. *Front Plant Sci* 6:267. <https://doi.org/10.3389/fpls.2015.00267>
- Liu J, Pang X, Cheng Y, Yin Y, Zhang Q, Su W, Hu B, Guo Q, Ha S, Zhang J, Wan H (2018) The *Hsp70* gene family in *Solanum tuberosum*: genome-wide identification, phylogeny, and expression patterns. *Sci Rep* 8:16628. <https://doi.org/10.1038/s41598-018-34878-7>
- Livak KJ, Schmittgen TD (2001) Analysis of relative gene expression data using real-time quantitative PCR and the 2<sup>-</sup>(Delta Delta C(T)). *Method Methods* 25:402–408. <https://doi.org/10.1006/meth.2001.1262>
- Love MI, Huber W, Anders S (2014) Moderated estimation of fold change and dispersion for RNA-seq data with DESeq2. *Genome Biol* 15:550. <https://doi.org/10.1186/s13059-014-0550-8>
- Luo Y, Pang D, Jin M, Chen J, Kong X, Li W, Chang Y, Li Y, Wang Z (2019) Identification of plant hormones and candidate hub genes regulating flag leaf senescence in wheat response to water deficit stress at the grain-filling stage. *Plant Direct* 3:e00152. <https://doi.org/10.1002/pld3.152>
- Merlot S, Gost F, DI G, Vavasseur A, Giraudat J (2001) The ABI1 and ABI2 protein phosphatases 2C act in a negative feedback

- regulatory loop of the abscisic acid signalling pathway. *Plant J* 25:295–303. <https://doi.org/10.1046/j.1365-313x.2001.00965.x>
- Miller G, Shulaev V, Mittler R (2008) Reactive oxygen signaling and abiotic stress. *Physiol Plant* 133:481–489. <https://doi.org/10.1111/j.1399-3054.2008.01090.x>
- Moon J, Zhu L, Shen H, Huq E (2008) PIF1 directly and indirectly regulates chlorophyll biosynthesis to optimize the greening process in *Arabidopsis*. *Proc Natl Acad Sci USA* 105:9433–9438. <https://doi.org/10.1073/pnas.0803611105>
- Nambara E, Marion-Poll A (2005) Abscisic acid biosynthesis and catabolism. *Annu Rev Plant Biol* 56:165–185. <https://doi.org/10.1146/annurev.arplant.56.032604.144046>
- Nieto-Sotelo J, Martínez LM, Ponce G, Cassab GI, Alagón A, Meeley RB, Ribaut JM, Yang R (2002) Maize HSP101 plays important roles in both induced and basal thermotolerance and primary root growth. *Plant Cell* 14:1621–1633. <https://doi.org/10.1105/tpc.010487>
- Oh E, Kang H, Yamaguchi S, Park J, Lee D, Kamiya Y, Choi G (2009) Genome-wide analysis of genes targeted by PHYTOCHROME INTERACTING FACTOR 3-LIKE5 during seed germination in *Arabidopsis*. *Plant Cell* 21:403–419. <https://doi.org/10.1105/tpc.108.064691>
- Ohama N, Sato H, Shinozaki K, Yamaguchi-Shinohara K (2017) Transcriptional regulatory network of plant heat stress response. *Trends Plant Sci* 22:53–65. <https://doi.org/10.1016/j.tplants.2016.08.015>
- Park E, Kim T-H (2017) Production of ABA responses requires both the nuclear and cytoplasmic functional involvement of PYR1. *Biochemical and Biophysical Res Commun* 484:34–39. <https://doi.org/10.1016/j.bbrc.2017.01.082>
- Perez-Amador MA (2002) Induction of the arginine decarboxylase ADC2 gene provides evidence for the involvement of polyamines in the wound response in *Arabidopsis*. *Plant Physiol* 130:1454–1463. <https://doi.org/10.1104/pp.009951>
- Pietrocola F, Izzo V, Niso-Santano M, Vacchelli E, Galluzzi L, Maiuri MC, Kroemer G (2013) Regulation of autophagy by stress-responsive transcription factors. *Semin Cancer Biol* 23:310–322. <https://doi.org/10.1016/j.semcancer.2013.05.008>
- Prasad BD, Goel S, Krishna P (2010) In silico identification of carboxylate clamp type tetratricopeptide repeat proteins in *Arabidopsis* and rice as putative co-chaperones of Hsp90/Hsp70. *PLoS ONE* 5:e12761. <https://doi.org/10.1371/journal.pone.0012761>
- Qi C, Lin X, Li S, Liu L, Wang Z, Li Y, Bai R, Xie Q, Zhang N, Ren S, Zhao B, Li X, Fan S, Guo YD (2019) SoHSC70 positively regulates thermotolerance by alleviating cell membrane damage, reducing ROS accumulation, and improving activities of antioxidant enzymes. *Plant Sci* 283:385–395. <https://doi.org/10.1016/j.plantsci.2019.03.003>
- Qian Y, Cao L, Zhang Q, Ameer M, Chen K, Chen L (2020) SMRT and Illumina RNA sequencing reveal novel insights into the heat stress response and crosstalk with leaf senescence in tall fescue. *BMC Plant Biol* 20:366. <https://doi.org/10.1186/s12870-020-02572-4>
- Qu AL, Ding YF, Jiang Q, Zhu C (2013) Molecular mechanisms of the plant heat stress response. *Biochem Biophys Res Commun* 432:203–207. <https://doi.org/10.1016/j.bbrc.2013.01.104>
- Queitsch C, Hong SW, Vierling E, Lindquist S (2000) Heat shock protein 101 plays a crucial role in thermotolerance in *Arabidopsis*. *Plant Cell* 12:479–492. <https://doi.org/10.1105/tpc.12.4.479>
- Ray DK, Gerber JS, MacDonald GK, West PC (2015) Climate variation explains a third of global crop yield variability. *Nat Commun* 6:5989. <https://doi.org/10.1038/ncomms6989>
- Reinbothe C, Springer A, Samol I, Reinbothe S (2009) Plant oxylipins: role of jasmonic acid during programmed cell death, defence and leaf senescence. *FEBS J* 276:4666–4681. <https://doi.org/10.1111/j.1742-4658.2009.07193.x>
- Sagor GHM, Berberich T, Takahashi Y, Niitsu M, Kusano T (2012) The polyamine spermine protects *Arabidopsis* from heat stress-induced damage by increasing expression of heat shock-related genes. *Transgen Res* 22:595–605. <https://doi.org/10.1007/s11248-012-9666-3>
- Saleem MA, Malik W, Qayyum A, Ul-Allah S, Ahmad MQ, Afzal H, Amjid MW, Ateeq MF, Zia ZU (2021) Impact of heat stress responsive factors on growth and physiology of cotton (*Gossypium hirsutum* L.). *Mol Biol Rep* 48:1069–1079. <https://doi.org/10.1007/s11033-021-06217-z>
- Sato S, Kato N, Iwai S, Hagimori M (2002) Effect of low temperature pretreatment of buds or inflorescence on isolated microspore culture in *Brassica rapa* (syn. *B. campestris*). *Breeding Sci* 52:23–26. <https://doi.org/10.1270/jsbbs.52.23>
- Scharf KD, Berberich T, Ebersberger I, Nover L (2012) The plant heat stress transcription factor (Hsf) family: structure, function and evolution. *Biochim Biophys Acta* 1819:104–119. <https://doi.org/10.1016/j.bbagr.2011.10.002>
- Sedaghatmehr M, Thirumalaikumar VP, Kamranfar I, Marmagne A, Masclaux-Daubresse C, Balazadeh S (2019) A regulatory role of autophagy for resetting the memory of heat stress in plants. *Plant Cell Environ* 42:1054–1064. <https://doi.org/10.1111/pce.13426>
- Shan X, Wang J, Chua L, Jiang D, Peng W, Xie D (2011) The role of *Arabidopsis Rubisco activase* in jasmonate-induced leaf senescence. *Plant Physiol* 155:751–764. <https://doi.org/10.1104/pp.110.166595>
- Singh D, Singh CK, Taunk J, Jadon V, Pal M, Gaikwad K (2019) Genome wide transcriptome analysis reveals vital role of heat responsive genes in regulatory mechanisms of lentil (*Lens culinaris* Medikus). *Sci Rep* 9:12976. <https://doi.org/10.1038/s41598-019-49496-0>
- Song X, Liu G, Duan W, Liu T, Huang Z, Ren J, Li Y, Hou X (2014) Genome-wide identification, classification and expression analysis of the heat shock transcription factor family in Chinese cabbage. *Mol Genet Genom* 289:541–551. <https://doi.org/10.1007/s00438-014-0833-5>
- Takehisa H, Sato Y (2019) Transcriptome monitoring visualizes growth stage-dependent nutrient status dynamics in rice under field conditions. *Plant J* 97:1048–1060. <https://doi.org/10.1111/tbj.14176>
- Tan M, Cheng D, Yang Y, Zhang G, Qin M, Chen J, Chen Y, Jiang M (2017) Co-expression network analysis of the transcriptomes of rice roots exposed to various cadmium stresses reveals universal cadmium-responsive genes. *BMC Plant Biol* 17:194. <https://doi.org/10.1186/s12870-017-1143-y>
- Thatcher LF, Foley R, Casarotto HJ, Gao LL, Kamphuis LG, Melsner S, Singh KB (2018) The RNA polymerase II carboxyl terminal domain (CTD) phosphatase-Like1 (CPL1) is a biotic stress susceptibility gene. *Sci Rep* 8:13454. <https://doi.org/10.1038/s41598-018-31837-0>
- Trapnell C, Pachter L, Salzberg SL (2009) TopHat: discovering splice junctions with RNA-Seq. *Bioinformatics* 25:1105–1111. <https://doi.org/10.1093/bioinformatics/btp120>
- Trapnell C, Roberts A, Goff L, Pertea G, Kim D, Kelley DR, Pimentel H, Salzberg SL, Rinn JL, Pachter L (2012) Differential gene and transcript expression analysis of RNA-seq experiments with TopHat and cufflinks. *Nat Protoc* 7:562–578. <https://doi.org/10.1038/nprot.2012.016>
- Verma V, Ravindran P, Kumar PP (2016) Plant hormone-mediated regulation of stress responses. *BMC Plant Biol* 16:86. <https://doi.org/10.1186/s12870-016-0771-y>
- Wang Y, Lin S, Song Q, Li K, Tao H, Huang J, Chen X, Que S, He H (2014) Genome-wide identification of heat shock proteins (Hsps) and Hsp interactors in rice: Hsp70s as a case study. *BMC Genom* 15:344. <https://doi.org/10.1186/1471-2164-15-344>

- Wang A, Hu J, Huang X, Li X, Zhou G, Yan Z (2016) Comparative transcriptome analysis reveals heat-responsive genes in Chinese cabbage (*Brassica rapa* ssp. *chinensis*). *Front Plant Sci* 7:939. <https://doi.org/10.3389/fpls.2016.00939>
- Wasternack C (2007) Jasmonates: an update on biosynthesis, signal transduction and action in plant stress response, growth and development. *Ann Bot* 100:681–697. <https://doi.org/10.1093/aob/mcm079>
- Wijewardene I, Mishra N, Sun L, Smith J, Zhu X, Payton P, Shen G, Zhang H (2020) Improving drought-, salinity-, and heat-tolerance in transgenic plants by co-overexpressing *Arabidopsis* vacuolar pyrophosphatase gene *AVP1* and *Larrea* Rubisco activase gene *RCA*. *Plant Sci* 296:110499. <https://doi.org/10.1016/j.plantsci.2020.110499>
- Wu Y, Xu J, Han X, Qiao G, Yang K, Wen Z, Wen X (2020) Comparative transcriptome analysis combining SMRT- and Illumina-based RNA-Seq identifies potential candidate genes involved in betalain biosynthesis in Pitaya fruit. *Int J Mol Sci* 21:3288. <https://doi.org/10.3390/ijms21093288>
- Xie L, Dong C, Shang Q (2019) Gene co-expression network analysis reveals pathways associated with graft healing by asymmetric profiling in tomato. *BMC Plant Biol* 19:373. <https://doi.org/10.1186/s12870-019-1976-7>
- Xu J, Xue C, Xue D, Zhao J, Gai J, Guo N, Xing H (2013) Overexpression of GmHsp90s, a heat shock protein 90 (Hsp90) gene family cloning from soybean, decrease damage of abiotic stresses in *Arabidopsis thaliana*. *PLoS ONE* 8:e69810. <https://doi.org/10.1371/journal.pone.0069810>
- Young MD, Wakefield MJ, Smyth GK, Oshlack A (2010) Gene ontology analysis for RNA-seq: accounting for selection bias. *Genome Biol* 11:R14. <https://doi.org/10.1186/gb-2010-11-2-r14>
- Yu X, Wang H, Lu Y, de Ruiter M, Cariaso M, Prins M, van Tunen A, He Y (2012) Identification of conserved and novel microRNAs that are responsive to heat stress in *Brassica rapa*. *J Exp Bot* 63:1025–1038. <https://doi.org/10.1093/jxb/err337>
- Zhang L, Cai X, Wu J, Liu M, Grob S, Cheng F, Liang J, Cai C, Liu Z, Liu B, Wang F, Li S, Liu F, Li X, Cheng L, Yang W, Li MH, Grossniklaus U, Zheng H, Wang X (2018a) Improved *Brassica rapa* reference genome by single-molecule sequencing and chromosome conformation capture technologies. *Hortic Res* 5:50. <https://doi.org/10.1038/s41438-018-0071-9>
- Zhang S, Wang S, Lv J, Liu Z, Wang Y, Ma N, Meng Q (2018b) SUMO E3 ligase SIZ1 facilitates heat tolerance in tomato. *Plant Cell Physiol* 59:58–71. <https://doi.org/10.1093/pcp/pcx160>
- Zhou J, Wang J, Cheng Y, Chi YJ, Fan B, Yu JQ, Chen Z (2013) NBR1-mediated selective autophagy targets insoluble ubiquitinated protein aggregates in plant stress responses. *PLoS Genet* 9:e1003196. <https://doi.org/10.1371/journal.pgen.1003196>
- Zhou J, Wang J, Yu JQ, Chen Z (2014) Role and regulation of autophagy in heat stress responses of tomato plants. *Front Plant Sci* 5:174. <https://doi.org/10.3389/fpls.2014.00174>

**Publisher's Note** Springer Nature remains neutral with regard to jurisdictional claims in published maps and institutional affiliations.